INVESTIGATION OF THE EFFECTOR ROLE OF IPAD FROM THE TYPE III SECRETION SYSTEM OF *SHIGELLA FLEXNERI*

By

Olivia Arizmendi Perez

Submitted to the graduate degree program in the Department of Molecular Biosciences and the Graduate Faculty of the University of Kansas in partial fulfillment of the requirements for the degree of Doctor of Philosophy.

_____

Chairperson: Wendy L. Picking, Ph.D.

_____

William D. Picking, Ph.D.

_____

Mark L. Richter, Ph.D.

_____

Roberto N. De Guzman, Ph.D.

_____

Josephine R. Chandler, Ph.D.

_____

Thomas J. Tolbert, Ph.D.

Date Defended: April 28, 2016

The Dissertation Committee for Olivia Arizmendi Perez

certifies that this is the approved version of the following dissertation:

INVESTIGATION OF THE EFFECTOR ROLE OF IPAD FROM THE TYPE III SECRETION SYSTEM OF *SHIGELLA FLEXNERI*

_____

Chairperson: Wendy L. Picking, Ph.D.

Date approved: April 28, 2016

Abstract

Shigellosis is an infectious gastrointestinal disease caused by *Shigella* spp. Approximately 165 million cases of shigellosis occur every year around the world, the vast majority of them in developing countries. High levels of antibiotic resistance, an increase in multidrug-resistant *Shigella* isolates and the lack of a licensed vaccine are factors that situate shigellosis as a public health problem, especially among young children. *Shigella* is able to cause death of resident macrophages in the gut to avoid bacterial clearance early after infection. *Shigella* is then able to colonize the intestinal epithelium and induce inflammation, which ultimately gives rise to the symptoms of dysentery and bacterial shedding. The virulence of *Shigella* is intimately tied to its Type III Secretion System (T3SS) for which invasion plasmid antigen D (IpaD) is a structural element. Previous studies have established that IpaD is secreted at levels beyond what is needed for its role as the T3SS needle tip protein. Furthermore, IpaD was recently shown to induce apoptosis in B lymphocytes in conjunction with an additional unknown factor. The projects presented in this dissertation aim to identify the role of IpaD as a secreted effector in the pathogenesis of *Shigella*. We have studied the effect of IpaD in macrophages and epithelial cells through a multidisciplinary approach using cell biology, immunology and protein biochemistry. Our findings indicate that IpaD plays a role in the development of an apoptotic pathway in macrophages. *In vitro*, macrophages incubated with recombinant IpaD undergo activation of caspases, damage to mitochondria and decreased cellular integrity. Furthermore, *Shigella* infection of cultured macrophages showed that IpaD is responsible of a portion of the cell death caused by the bacterium. These findings allow us to conclude IpaD is responsible for a portion of the macrophage cell death during *Shigella* infection.

Acknowledgements

I would like to thank Dr. Wendy Picking for this journey. I am grateful for the wonderful opportunities she has given me, especially the opportunity to resume my research career and her encouragement on applying to a graduate program. I particularly enjoyed learning other aspects of academic science, such as grant writing, and all the meetings and conferences I participated on thanks to her support. Above all, I want to thank her for allowing me to follow my own path.

I want to also thank Dr. Bill Picking, for reading my drafts, for listening to my ideas. And because he also believed in me many years ago. Thank you to all my committee members, Dr. Mark Richter, Dr. Roberto de Guzman, and Dr. Tom Tolbert for helping me achieve this tremendous task. Special thanks to Dr. Josie Chandler who was always both encouraging and insightful.

Thank you to all the members of my lab, both former and current. To those that I count as my friends, Phil, Shyamal, Prashant and Melissa, without you, this would have been 100x more difficult. To all the amazing undergrads who I had the joy and privilege to mentor: Micah, Lindsey, Jordan, Katie. With each one of you I learned so much. I am glad to see Universities training wonderful women scientists every day.

To my alma mater, UNAM, for the excellent education I received. *Por mi raza hablará el espíritu*. To my undergrad mentor Dr. Imelda López-Villaseñor, for seeing in me something that I could not at that time. Because I carry with me all her teachings, both professional and personal.

Finally, this was only possible because I always had the love of my family to carry me through. My husband Francisco, our girls Nicole and Dixie. For the long nights I spent doing homework, or writing a paper. It is my husband's love that showed me I could be and do anything I wanted. Thank you Paco, for being the home I never had and the best example of how to be true to oneself.

Lastly, I want to thank Lupita and Paco, for all their encouragement and their love. Thank you to Marisol, Víctor, Mar and Miguel, for being my family and for showing me how to be strong.

TABLE OF CONTENTS

LIST OF FIGURES

LIST OF TABLES

CHAPTER I: Historical Review

Diarrheal disease burden

Diarrheal diseases are caused by pathogenic bacteria, viruses or parasites entering through the gastrointestinal tract through water, food or objects contaminated with stools[1]. The global burden of diarrheal diseases has been calculated as 1.7 billion cases per year. In 2010, it was estimated that approximately 10% of deaths in children under the age of five were due to diarrhea, the second leading cause of death in that population[2]. Mortality caused by diarrhea is higher than all deaths caused by AIDS, malaria and measles combined[3]. Malnourished children, as well as HIV-infected individuals, are at an increased risk of dying from diarrheal disease[4].

Inadequate or nonexistent sanitation, poor hygiene and contaminated water sources are common causes of diarrheal disease in developing countries[1,4,5]. Children in these countries have, on average, three diarrheal episodes per year[6]. In industrialized countries, diarrheal disease outbreaks are usually self-limiting and are commonly the result of contamination of a food source[7]. Foodborne illnesses in the US are estimated at 48 million cases per year. Hospitalizations and deaths due to foodborne illness are primarily seen in infants, elderly or immunocompromised individuals[8].

Shigella epidemiology

Shigellosis is a diarrheal disease caused by gram-negative bacteria in the *Shigella* genus. *Shigella* is transmitted through the oral-fecal route and causes symptoms that include abdominal cramps, tenesmus and diarrhea with blood and mucus. If not quickly treated, shigellosis can lead to death. The global burden of shigellosis has been estimated at 165 million cases with 600,000 deaths per year[9]. Recent reports indicate that shigellosis-related deaths are decreasing[10]. Nevertheless,

Shigella remains a public health problem in developing regions of the world where poor sanitation and reduced access to health care affects vulnerable populations and hinders child development. Children under five years of age are considered most-at-risk for shigellosis and this population carries the additional burden of malnutrition, seizures, and stunted growth caused by the infection[11].

Several approaches are being explored to control the global effects of shigellosis. For example, diarrheal disease is six times less likely in breast-fed infants, due to the antimicrobial factors found in breast milk and the exclusion of contaminated water intake[12]. Flies are known mechanical vectors for the spread of shigellosis, and have been found to carry the pathogen for up to 20 days[13,14], therefore, improved sanitation and domestic hygiene could decrease the incidence of shigellosis as well as other causes of childhood diarrhea[15]. However, behavior modification and proper infrastructure are needed for the success of these control measures[12]. Development of vaccines against shigellosis has been a main focus in the battle against this infection. Several vaccine candidates are in pre-clinical or clinical phases of development and comprise live-attenuated, whole-killed and subunit vaccines[16–20].

Shigella sonnei is responsible of 72% of total cases of shigellosis in the US, with 30% of those traced to contaminated food[21]. Outbreaks of multidrug resistant bacteria are usually daycare center-associated[22]. Other industrialized countries show similar trends[23,24]. As a nation undergoes industrialization and improves its economic development *S. sonnei* becomes the predominant cause of shigellosis[25]. *Shigella flexneri* is predominantly seen in the developing world. Shigellosis is endemic in some countries in Latin America, East Africa, the Indian subcontinent[26–28]. *S. dysenteriae* serotype 1 is associated with the highest severity of symptoms and is found intermittently in epidemics in Sub-Saharan Africa and South Asia[29]. An outbreak in Sierra Leone

had an overall case fatality rate of 3.1%, and of 6.1% in children under 5[30]. Several outbreaks have been linked to refugee settlements[31].

Shigella biology

Shigella is a genus of gram-negative bacteria that are non-motile, facultative anaerobic, rod-shaped, non-sporulating, non-lactose-fermenting[32]. The *Shigella* genus comprises four different species: *S. dysenteriae, S. flexneri, S. boydii* and *S. sonnei* (also known as serogroups A through D). All species share approximately 80-85% of their genome[33], and have been distinctly classified as a separate clade from *Escherichia coli* despite their phylogenetic closeness[34].

Variations in the O-antigen, a component of the cell envelope lipopolysaccharide (LPS), determine serotype classification in *Shigella*. There are at least 50 different serotypes (*S. dysenteriae,* 15; *S. flexneri,* 14; *S. boydii,* 20; and *S. sonnei,* 1). Serotype conversion occurs as a result of infection by bacteriophages that carry O-antigen modification genes[35,36].

Shigella is a human pathogen and can infect with doses as low as 10 to 200 organisms, likely due to a high acid tolerance that allows these bacteria to survive the gastric environment[37]. Some *Shigella* serotypes have been identified as the cause of dysentery outbreaks in captive primates in zoo and laboratory environments[38,39]. *Shigella* is typically identified by microbiological isolation and analysis of fecal samples. Identification is achieved through culture in selective media such as MacConkey agar, xylose lysine deoxycholate agar and Salmonella-Shigella agar. Serological testing is further performed for correct diagnosis[40].

Free-living amoeba have been studied as environmental hosts for *Shigella*. *S. sonnei* and *S. dysenteriae* were able to grow and persist inside *Acanthamoeba castellanni*[41,42], whereas *S. flexneri* was found to kill the amoeba by necrosis[43]. These observations could explain the geographical

distribution of different *Shigella* species, although further studies are needed to better understand this association.

Antibiotic resistance in *Shigella* is now a major cause of concern around the world. Recent reports indicate that multidrug resistant strains are more commonly isolated and several mechanisms of resistance have been identified such as mutations in DNA gyrases and topoisomerases, which are common antibiotic targets. Resistance has been identified for fluoroquinolones, cephalosporins, tetracycline, gentamicin, chloramphenicol and sulfonamides[44,45]. In a multi-state outbreak in 2014-2015, the Centers for Disease Control and Prevention (CDC) issued a report stating that 90% of the clinical isolates linked to the outbreak were resistant to ciprofloxacin, the drug of choice against shigellosis in the US[46].

Complications of shigellosis

Fatal complications of shigellosis include intestinal perforation, toxic megacolon, hemolytic-uremic syndrome and septicemia[47]. Toxic megacolon is an acute severe colitis in which the colon is distended and paralyzed. It can lead to rupture of the colon and subsequent peritonitis. Toxic megacolon has also been documented in a case of sexual transmission of *S. sonnei*[48]. Bacteremia can be the result of an ulcerated colonic mucosa and is more commonly seen in malnourished or immunocompromised individuals[49,50]. Hemolytic-uremic syndrome (HUS) is a severe complication that can lead to acute renal failure with hyperkalemia, severe hemolytic anemia and thrombocytopenia. HUS is mainly caused by the Shiga toxin secreted by *S. dysenteriae* type 1, although LPS has also been found to cause it. It is the leading cause of death in *S. dysenteriae* type 1 outbreaks, with a 36% case-fatality rate[51].

Other non-fatal complications of shigellosis have also been identified. Reiter's syndrome is a type of reactive arthritis (ReA) found after bacterial infections. It is unclear exactly how *Shigella* is causative of ReA but molecular mimicry, in which an epitope of the bacterium mimics that of a self-antigen, has been proposed[52]. Other investigators propose aberrant HLA interactions with *Shigella* peptides would cause ReA in individuals with other ongoing inflammatory processes[53]. Post-infectious irritable bowel syndrome can also be caused by shigellosis after the acute colitis caused by the disease[54]. Furthermore, individuals with Crohn's disease are at an elevated risk of infection with *Shigella*[55].

Pathogenesis

Shigella reaches the colon after ingestion of contaminated food or water by an individual. In the intestinal lumen, *Shigellae* organisms are unable to invade enterocytes through the apical side and are transcytosed by microfold cells (M cells) of the colonic epithelium[56]. M cells present the pathogen to resident macrophages as an initial immune response to the infection, however, *Shigella* prompts resident macrophages to die in order to avoid bacterial clearance by these phagocytes. Apoptotic cell death has been observed in macrophages at the lamina propria of mucosal biopsies[57] and apoptotic macrophages, T and B cells have been found in the lymphoid follicles of rabbits infected with *Shigella*[58]. Furthermore, several studies have shown evidence of different types of cell death occurring in these immune cells, namely oncosis and necrosis[59–61].

Pyroptosis of macrophages mediated by *Shigella* has also been studied[62]. Pyroptosis is a type of inflammatory cell death that is caused by the activation of caspase-1 or caspase-11 and the subsequent release of pro-inflammatory cytokines IL-1β and IL-18[63]. It has been proposed that endolysosomal potassium channels formed by IpaB are the necessary signal for activation of the canonical inflammasome IPAF (NLRC4) and subsequent activation of caspase-1[64]. LPS of

intracellular *Shigella* sensed by the host has also been shown to trigger activation of a non-canonical inflammasome containing caspase-11 and gasdermin D[65]. The *Shigella* proteins MxiI and MxiH have been identified as activators of other inflammasome pathways[66,67].

After *Shigella* kills the resident macrophage by any of the pathways proposed, it is now at the basal side of the colon. *Shigella* then colonizes the intestinal epithelium by a trigger mechanism, in which effector proteins injected into the host cell elicit cytoskeletal rearrangements that lead to bacterial uptake[68]. Bacteria engulfed by epithelial cells are trapped inside a vacuole, which they rapidly lyse. Using an actin-dependent mechanism, they move about the invaded epithelial cell and spread through lateral movement to neighboring enterocytes[69]. Bacterial shedding and diarrheal symptoms are due to *Shigella*-induced necrosis of invaded enterocytes and the ensuing inflammatory response of the host.

Type III secretion system

The infective cycle described for *Shigella* is dependent on a functional Type III Secretion System (T3SS). Type III Secretion Systems are macromolecular assemblies utilized by gram-negative bacteria to deliver proteins from their cytoplasm into the host cell or to the extracellular environment[69]. *Shigella* carries large virulence plasmids such as pINV A or pINV B[70], which contain the genes encoding the T3SS of these organisms. Loss of the plasmid thus converts *Shigella* to an avirulent state[71]. The plasmid pINV is 220-260 kb in size and contains a highly conserved 31 kb region denominated 'entry region', which encodes proteins necessary for invasion of epithelial cells by *Shigella*[72], as well as intracellular survival and intra- and intercellular spread. Among the proteins encoded by the entry region are invasion plasmid antigens (Ipa) B, C and D which form the translocon responsible for the delivery of effectors to the host cell cytoplasm.

The entry region of the virulence plasmid is divided into the *ipa* and *mxi-spa* loci, together these consist of 38 open reading frames (ORFs). The genes essential for assembly and functionality of the T3SS are the membrane expression of ipa (*mxi*) and the surface presentation of ipa (*spa*) genes. Expression of the structural components of the T3SS is activated at 37°C by a regulatory cascade between VirF, an AraC type transcriptional regulator[73], and VirB, an intermediate regulator that derepresses the T3SS operons[74]. Therefore, expression of the T3SS occurs in *Shigella* once inside the human body[75].

The Type III Secretion Apparatus (T3SA) of *Shigella* is composed of a basal body, a C-ring compartment, and a needle that together span the inner membrane, periplasm and outer membrane (**Fig. 1**). At the basal body, MxiG polymerizes into a ring that docks the T3SA onto the inner membrane towards the periplasm[76]. MxiC has been shown to interact with Spa47 and avoid the premature secretion of effectors[77]. Spa33 is located at the C-ring of the T3SA and interacts with Spa47, a cytoplasmic ATPase that powers secretion by the T3SA[78]. MxiN and MxiK are also located in the bacterial cytoplasm and are required for the transit of MxiI and MxiH, structural components of the T3SA needle[79,80]. MxiI is the inner rod component of the needle, whereas MxiH is the structural component that polymerizes onto an extracellular needle or rod. At the tip of the needle, IpaD forms a pentameric ring that closes the T3SA[81]. Acting as a molecular plug, IpaD controls the recruitment of IpaB for full maturation of the needle upon or prior to host cell contact[82]. The full formation of the translocon occurs upon interaction of IpaB with sphingomyelin and cholesterol in the host cell membrane, triggering recruitment of IpaC[83]. The chaperone IpgC associates with IpaB and IpaC in the intracellular compartment of the bacteria, and is released as each protein is secreted for translocon assembly[84]. The cytoplasmic MxiE/IpgC complex then activates the transcription of late effectors[85].

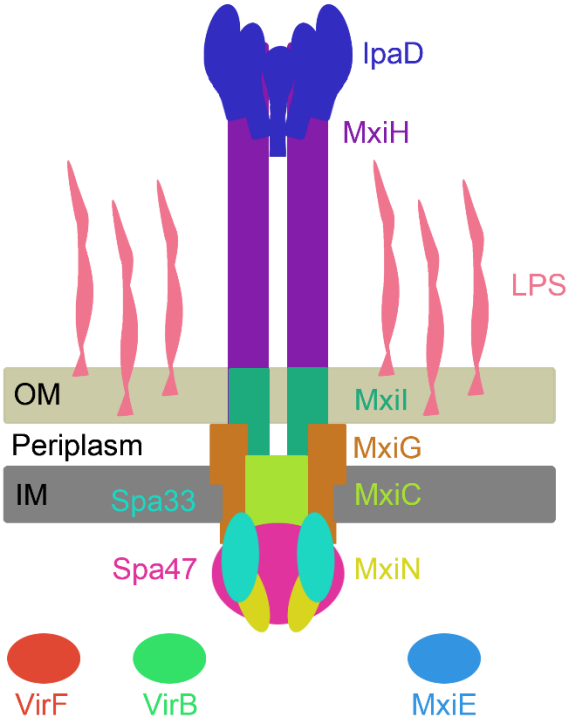

Fig. 1. *Shigella* type III Secretion System Apparatus (T3SA). The T3SA is formed by the basal body and C-ring that span the inner and outer membrane of the bacteria. The ATPase Spa47 is localized in the cytoplasm of the bacteria. The extracellular needle rod is a polymer of the protein MxiH. The needle tip is formed of a pentameric assembly of IpaD. The regulatory factors VirF, VirB and MxiE are also shown.

Invasion plasmid antigen D (IpaD)

Regulation of secretion

Invasion plasmid antigen D (IpaD) was first described as one of four antigens present in a *Shigella* virulent strain grown at 37°C. When serum from an infected monkey was used, the invasion plasmid antigens A through D were recognized through immunoblot in lysates from the virulent strain. The anti-serum failed to detect any proteins in lysates from avirulent strains[32]. IpaD is a 37 kDa hydrophilic protein that is encoded along with IpaA, IpaB, IpaC and IpgC in the locus *ipgC-ipaABCD* of the virulence plasmid. Proteins IpaB, IpaC and IpaD are stored in the cytoplasm in addition to their membrane-bound assemblies and released into the medium upon contact with

epithelial cells, or incubation in microtiter wells coated with certain extracellular matrix proteins[86]. Mutants with nonpolar disruptions of the *ipaB*, *ipaC* or *ipaD* genes are unable to invade. Moreover, mutation of IpaB or IpaD results in uncontrolled secretion in the absence of external stimuli[87].

Further investigation of the role of IpaD in T3SS function demonstrated that this protein is necessary for both protein secretion control and proper formation of the translocon[88]. Targeted mutations of certain regions in the *ipaD* gene established that the N-terminal portion of this protein is required for secretion control, but a central portion is necessary for invasion of host cells. Furthermore, it has been shown that IpaD itself is secreted upon proper stimulation [89,90]. Other studies showed that IpaD is surface exposed and localizes at the tip of the T3SA needle, where it interacts directly with the external rod protein MxiH[89,91]. Bile salts including deoxycholate (DOC) are found in abundance in the colonic lumen. DOC binds to IpaD and induces a conformational change in this protein[82]. This is thought to prompt IpaD to recruit IpaB at the top of the needle as the first step in the formation of the translocon.

Interaction with MxiC

MxiC is a T3SS protein that is found in the basal compartment of the T3SA. In the context of T3SS secretion, MxiC is known to associate indirectly with Spa47, blocking secretion from the T3SA. This role was found to regulate the secretion of late effectors such as IpaA, IpgD and IpaH. MxiC, however, did not prevent the structural assembly of IpaD at the tip of the needle or formation of the translocon as secretion of both IpaB and IpaC are unaffected by mutation of MxiC.

Association of IpaD with MxiC has been proposed. Mutants of IpaD denominated Class I mutants were found to display similar phenotypes of premature and non-responsive secretion as a MxiC mutant[92]. The authors elaborate on this finding as possible evidence of MxiC and IpaD interaction

in the bacterial cytoplasm and a regulatory role of IpaD independent of its role regulating the secretion of the translocon proteins IpaB and IpaC from the T3SA needle tip.

Binding to IpaB

Studies on the structure of IpaD indicate that this hydrophilic protein has a mainly α-helical structure with a dumbbell shape. It is comprised of a central coiled-coil, a distal domain and an N-terminal domain. The C-terminus of IpaD is necessary for proper interaction with MxiH and localization to the tip of the T3SA needle[93]. The N-terminal domain has been proposed as a self-chaperoning domain based on the fact that LcrV, the IpaD structural orthologue in *Yersinia* spp. lacks this domain and instead binds to chaperone LcrG in a similar way[94].

The IpaD distal domain has been implicated in the interaction of IpaD with IpaB, which is expected for proper T3SA tip assembly in preparation of the formation of the translocon upon recruitment of IpaC. The N-terminus of IpaB was shown to interact *in vitro* with the distal domain of IpaD, but only in the presence of DOC. IpaD undergoes a conformational change of its distal domain upon IpaB binding, which might resemble the events necessary for full T3SA maturation. *Shigella* mutants in the N-terminus of IpaB were defective in the localization of IpaB on the bacterial surface, rendering them deficient in contact hemolysis of erythrocytes and invasion of cultured cells[95].

Cell death

Finally, the first evidence of an effector role of IpaD in host cells was obtained through the investigation of apoptosis of B lymphocytes upon *Shigella* infection. IpaD was shown to be a TLR2 agonist in B lymphocytes. Along with an unidentified factor, IpaD is able to cause apoptosis

of these cells in what has been described as a novel pathway for immune system subversion by *Shigella*[96].

CHAPTER II: Materials and Methods

Materials: All reagent-grade chemicals were purchased from Thermo-Fisher Scientific, Waltham, MA or Sigma-Aldrich, St. Louis, MO unless otherwise indicated.

Cell lines HEK-293 (CRL-1573), HeLa (CCL-2), Henle I-407 (CCL-6), J774A.1 (TIB-67), RAW264.7 (TIB-71), U937 (CRL-1593.2) were from the American Type Culture Collection (ATCC), Manassas, VA. All cell culture media and supplements were from Mediatech, Manassas, VA. Glass-bottom plates were from MatTek, Ashland, MA. Accutase cell detachment solution and cytometer setup & tracking beads were from BD Biosciences, San Jose, CA.

Anti-β-actin (C-2), anti-vimentin (V9), anti-tubulinα (B-5-1-2) mouse monoclonals and anti-TOM20 (FL-145) rabbit polyclonal were from Santa Cruz Biotechnology, Santa Cruz, CA. Cleaved Caspase-3 Asp 175 (9661) antibody were from Cell Signaling Technology, Danvers, MA. IRDye 800CW Goat anti-Mouse IgG, IRDye 680RD Goat anti-Mouse IgG and Odyssey Blocking Buffer (TBS) were from LI-COR, Lincoln, NE. Trans-Blot Turbo RTA Mini Nitrocellulose Transfer Kit was from Bio-Rad, Hercules, CA.

The plasmids pET9a, pET15b, Clonables 2x Ligation Premix, *E. coli* NovaBlue cells, Tuner (DE3) cells were from Novagen, Madison, WI. QIAprep Spin Miniprep, QIAquick PCR Purification, QIAquick Gel Extraction kits, and Ni-NTA magnetic beads were from QIAGEN, Valencia, CA. All restriction endonucleases and TransPass COS/293 transfection reagent were from New England Biolabs, Ipswich, MA.

Alexa Fluor 488 goat anti-rabbit, Alexa Fluor 568 goat anti-mouse, Alexa Fluor 488 or 633 Phalloidin stain, DAPI, FlAsH-EDT2, FITC Annexin V/Dead Cell Apoptosis Kit, Hoechst, SlowFade gold reagent, Alexa Fluor 568 NHS Ester and live cell imaging solution were from Life

Technologies, Grand Island, NY. Recombinant Syrian hamster vimentin was from Cytoskeleton Inc., Denver, CO.

CytoTox 96 non-radioactive cytotoxicity assay kit and caspase luminescent substrates are from Promega, Madison, WI. Caspase inhibitors are from R&D Systems, Minneapolis, MN. Mouse T_h1/T_h2 9-plex ultra-sensitive kit was from Meso Scale Discovery, Rockville, MD. NucView 488 Caspase-3 assay kit, staurosporine and JC-1 mitochondrial membrane potential detection kit were from Biotium, Hayward, CA.

***Shigella* strains:** *Shigella flexneri* serotype 2a strain 2457T was a gift from Anthony T. Maurelli, Uniformed Services University of Health Sciences, Bethesda, MD. Philippe J. Sansonetti, Institut Pasteur, Paris, FR, provided SF620, SF621 and SF622 which contain nonpolar mutations in *ipaB*, *ipaC* and *ipaD* genes, respectively.

Buffers and Media: See Appendix A for buffer compositions, media and other recipes.

Bacterial strains and growth conditions: Antibiotic concentrations for both liquid and solid media growth were 100 µg/ml ampicillin (to select for pWPsf4 and pET-series constructs) and 34 µg/ml chloramphenicol (to select for pACYC constructs). Growth of liquid cultures was at 37°C with shaking at 200 RPM for *Shigella* and *Escherichia coli*. *Shigella* were grown on trypticase soy agar (TSA) plates containing 0.025% Congo red with appropriate antibiotics for selection of the virulence and complementation plasmids. Congo red is used as an indicator dye because it is known to bind to cells with an active T3SS, and is thus used as an indicator of virulence plasmid retention. Red colonies were inoculated into trypticase soy broth (TSB) containing 50 µg/ml of kanamycin and 100 µg/ml of ampicillin as necessary. TSB cultures were grown at 37°C with shaking at 200 rpm. *E. coli* was grown on LB plates. All solid media were incubated at 37°C.

Cloning of *ipaD* for expression: Plasmid *ipaD*/pWPsf4 was used as a template for PCR reactions intended to clone the *ipaD* gene for overexpression in *E. coli*. The plasmid was digested with NdeI and BamHI for isolation of the *ipaD* gene and ligated into NdeI/BamHI digested pET9a. The resulting plasmid *ipaD*/pET9a was used for recombinant protein production. A humanized *ipaD* gene was purchased from Integrated DNA Technologies, Coralville, IA and cloned into pTandem-1 immediately downstream of a Kozak sequence containing the NcoI restriction site. Correct orientation and codon frame were verified by DNA sequencing. The resulting plasmid Humanized-*ipaD*/pTandem-1 was used for expression of IpaD in transfected epithelial cells.

Growth and recombinant expression of proteins: *ipaD*/pET9a was transformed into Tuner (DE3) competent *E. coli* cells and grown on a Luria-Bertani (LB) plate containing kanamycin and incubated overnight. A single colony was grown in 10 ml LB containing kanamycin to generate a permanent stock (200 µl 50% glycerol plus 1 ml broth culture) which was stored at -80°C. This permanent stock was used to start an overnight 10 ml culture in LB media, and 1-2 ml of the overnight culture was used to inoculate each liter of auto-induction media (AI; see Appendix A). Cultures were grown overnight (~16 hr) at 37°C with shaking at 200 RPM. Protein expression was induced by the depletion of glucose in the media and the intake of lactose. The cells were harvested by centrifugation at 4°C. The cell pellet was resuspended in Q binding buffer (see Appendix A). The cells were sonicated and the solution clarified by centrifugation at 20,000g for 20 mins. IpaD was purified in its soluble form from the *E. coli* cytoplasm. After centrifugation the supernatant fraction was applied to an anion-exchange Hi-Trap Q FF column. The protein was eluted with Q elution buffer (see Appendix A). The fractions containing the protein of interest, as determined by separation on a 12% SDS-PAGE gel, were collected. Fractions containing recombinant protein were pooled and dialyzed into PBS, pH 7.4 (ÄKTA purification method in Appendix C).

Production of protein lysates: Epithelial or macrophage cell lines were incubated at 37°C in a 5% CO_2 controlled environment. After various different treatments, protein lysates were obtained by incubation of the cell monolayers with RIPA buffer with an appropriate protease inhibitor cocktail. Samples were boiled, run on a 12 or 15% SDS-PAGE gels and stained with Oriole fluorescent gel stain. Protein concentration was measured with a BCA assay. Protein determination buffer was prepared by adding 1 ml of Copper Sulfate Pentahydrate 4% solution to 49 ml of a Bicinchoninic Acid (BCA) solution. A standard curve was prepared from bovine serum albumin (BSA) dilutions into RIPA buffer. 50 µl of the standards or experimental samples were loaded onto a 96-well plate and 200 µl of protein determination buffer added. Plate was incubated for 30 minutes at 37°C. Then, plate was allowed to cool to room temperature and absorbance at 562 nm was measured using a Spectramax plate reader from Molecular Devices, Sunnyvale, CA. Protein concentration was determined by linear regression using the standard values.

Western blot analysis: Proteins were electrophoretically separated by standard acrylamide SDS-PAGE gel. After that, the proteins were electrophoretically transferred from SDS-PAGE gels to PVDF or nitrocellulose membranes using a Trans-Blot SD Semi-Dry Transfer Cell for 45 min at a constant voltage of 15V. After transfer, the membrane was incubated in blocking buffer with shaking for at least 1 hour at room temperature. The blocked membrane was then incubated with a solution containing primary antibodies. The primary antibody solution was allowed to incubate with the membrane at room temperature for at least 1 hour with gentle shaking. Following this incubation step, the membrane was rinsed three times with PBS or TBS containing 0.1%Tween-20 for 5 min. The membrane was incubated in the secondary antibody solution for 1 hour at room temperature with continuous shaking. The membrane was then rinsed three times with PBS or TBS

containing 0.1%Tween-20 for 5 min, and then rinsed. The blot was examined in an ODYSSEY Infrared Imaging System from LI-COR Biosciences.

Gentamicin Protection Assay: Confluent HeLa cell layers were used to seed 24-well plates 24 hours prior to inoculation with bacteria. Wild-type *Shigella* and *ipaD* mutant strains were streaked onto trypticase soy agar containing 0.025% Congo red (TSA-CR) and 100 µg/ml ampicillin one day prior to the assay. Five isolated colonies were inoculated into 10 ml of trypticase soy broth containing 100 µg/ml ampicillin and 50 µg/ml kanamycin. Cultures were grown to an A600 of ~0.5. While the cultures are growing, the HeLa cells were washed with serum-free DMEM containing 0.45% glucose to remove antibiotics. Three µl of bacteria were added to the HeLa cells and the 24-well plate was centrifuged at room temperature at 2000 x g for 5 min. The centrifugation step facilitates contact between the HeLa cells and the bacteria. The bacteria were incubated with the HeLa cells for 30 min at 37°C. The media was aspirated and the cells washed 3x with DMEM containing 5% calf serum and 50 µg/ml gentamicin, and then incubated for 2 hours in the gentamicin-containing media. After the 2 hour incubation, the cells were washed with DMEM and then overlaid with 0.5% agar to lyse the cells, followed by an overlay with 2x LB agar. The 24-well plates were incubated overnight at 37°C and colonies representing invasive bacteria were counted.

Chloroquine resistance assay: A modified gentamicin protection assay was in J774 macrophages. Cells were seeded at 2.5 × 105 per well in 24-well plates 24 hour prior to infection. Cells were then infected at an MOI of 10:1 with bacteria grown as above. Plate was centrifuged at room temperature at 250 x g for 4 min. The bacteria were incubated with the macrophages for 30 min at 37°C. The media was aspirated and the cells washed 3x with DMEM containing 50 µg/ml gentamicin. Cells were incubated for 2 hours at 37°C in DMEM containing 50 µg/ml gentamicin,

with or without 400 µM chloroquine. After the 2 hour incubation, the cells were washed with PBS three times and lysed in a 0.9% NaCl, 0.2% Triton X-100 solution. Lysates were serially diluted and plated onto TSA-CR. Colony forming units (CFU) were counted after a 16 hour incubation at 37°C. Percent cytosolic bacteria was quantified by (CFU in gentamicin plus chloroquine/CFUs in gentamicin) x 100.

Contact-Mediated Hemolysis: *ipaD* mutants were grown overnight on TSA-CR and inoculated into 10 ml of trypticase soy broth containing 100 µg/ml ampicillin and 50 µg/ml kanamycin. The bacteria were grown to an A600 of 0.5, pelleted at 3000 x g, and resuspended with 200 µl phosphate-buffered saline (PBS). Three ml defibrinated sheep blood from Colorado Serum, CO was diluted with 40 ml PBS and centrifuged to collect the red blood cells (RBCs). RBCs were resuspended in 3 ml PBS and 50 µl/well distributed to a 96-well plate. A 50 µl aliquot of each mutant strain was added to each of three wells, and then the 96-well plate was centrifuged at 2200 x g for 15 min at room temperature. The plate was incubated at 37°C for 1 hour. The bacteria were sheared from the RBCs by vigorously resuspending the pellet in each well with 100 µl of ice-cold PBS. The plate was again centrifuged at 2200 x g for 15 min at 10°C. 100 µl of the supernatant from each well was transferred to a fresh well and the released hemoglobin measured by the absorbance at 545 nm using a Spectramax plate reader.

Overnight Secretion: A 10 ml culture of each *ipaD* mutant was grown as above, except the culture was incubated overnight. Bacteria were pelleted by centrifugation at 3000 x g and the supernatant was transferred to a 30 ml Corex centrifuge tube on ice. The bacterial pellet was resuspended in 1 ml of water and frozen. One ml of 100% TCA was mixed into the bacterial supernatant, followed by a one hour incubation on ice. The samples were then centrifuged at 11,800 x g for 15 min. The samples were washed with ice-cold 5% TCA and centrifuged as above. Next, the samples were

washed twice with ice-cold acetone. After the final wash, the Corex tubes were inverted and the acetone completely evaporated. Once dry, the pellets were resuspended with 400 µl PBS plus 200 µl 3x SDS-PAGE sample buffer plus 20 µl 1.5 M dithiothreitol (DTT). For quantitative purposes, the secreted proteins were analyzed by Western blot.

Congo Red Induced Secretion: Bacterial cultures were grown as indicated above to mid-log phase, harvested, and resuspended in 1 ml PBS. CR (10 mg/ml) was added to a final concentration of 1 mg/ml and incubated for 15 min at 37°C. The supernatants were clarified, the secreted proteins separated by SDS-PAGE and finally transferred to PVDF for Western blot analysis.

Fluorescence Labeling of IpaD: To facilitate optimal labeling, IpaD was concentrated to at least 2 mg/ml prior to labeling. Enough Alexa 568 NHS ester to provide at least a 10-fold molar excess to IpaD was dissolved in a minimal amount of dimethylformamide (DMF). At least 2 mg of IpaD was aliquoted to a small test tube, along with a 0.25 inch stir bar. The following steps were performed at room temperature while stirring. Alexa dye was added dropwise to IpaD and the test tube was purged with N2 for 10 min to remove molecular oxygen. The labeling reaction was then sealed with paraffin paper and incubated for 2 hours. Free dye was removed from IpaD by overnight dialysis onto PBS and a purification step in a Pierce dye removal column.

Concentrations were determined for the Alexa-labeled protein using UV-Vis absorbance spectroscopy. The A280 must be corrected to account for the absorbance of light at 280 nm by the fluorescent probe. The A280 and A575 of Alexa-labeled protein were collected. The A280 was corrected using the following equation:

$$A280\ Observed - (CF * A575) = A280\ Actual$$

Where CF (CF = 0.46) is the correction factor for Alexa 568, A280 Observed is the experimentally determined absorbance at 280 nm, A575 is the experimentally determined absorbance at 575 nm, and A280 Actual is the absorbance at 280 nm corrected for Alexa dye absorbance. A280 Actual was used to calculate the protein concentration using the Beer-Lambert Law:

$$A = \varepsilon c l$$

where A represents the absorbance value, ε represents the molar extinction coefficient, c represents the molar concentration, and l is the path length of the cuvette (1 cm). ε for IpaD is 36,900 M^{-1} cm^{-1}.

The degree of labeling (DOL) was calculated using the following equation:

Alexa concentration (M) / Protein concentration (M) * 100 = DOL (%)

Far-UV Circular Dichroism: Far-UV circular dichroism (CD) spectra were collected with a Jasco J815 spectropolarimeter equipped with a Peltier temperature controller from Jasco Inc, Easton, MA. IpaD at a concentration of 0.3 mg/ml was loaded into a 0.1 cm path length cuvette and spectra were collected at 10°C. A resolution of 1.0 nm was employed with a scanning speed of 50nm/min and a 2 sec data integration time.

Transient Transfections of HEK-293 cells: Humanized-*ipaD*/pTandem-1 was transiently transfected into HEK-293 cells using TransPass COS/293 transfection reagent in DMEM. Cells were plated one day before transfection in a 6-well plate so that cells would be 70% confluent at the time of transfection. TransPass reagent was prepared by diluting the appropriate amount in 1 ml of serum-free DMEM (6 µl TransPass / 3 µg DNA). The DNA:transfection reagent mix was gently mixed and incubated for 30 min at room temperature to allow for complex formation. DNA-

TransPass complexes were then added drop-wise to each well. The plate was then rocked for 10 min at room temperature, and later incubated at 37°C, 5% CO_2 for 6-48 hours.

Immunofluorescence microscopy: Transfected HEK-293 cells, which had been grown in coverslips inside a 6-well plate well, were fixed with 4% paraformaldehyde in PBS for 30 min at room temperature. The fixed cells were then rinsed with 10 mM glycine, 10% BSA in PBS for 10 min to neutralize the fixative. Cells were permeabilized with an incubation in 0.25% Triton X-100 in PBS for 15 min, and blocked in 10% BSA in PBS for 1 hour at room temperature. After the blocking buffer was removed, a 1:1000 solution of primary antibody in 10% BSA in PBS was applied and allowed to incubate for 2 hours at room temperature. Coverslips were rinsed with PBS three times and a 1:1000 secondary antibody solution allowed to incubate for 1 hour at room temperature. F-actin was stained with Alexa-labeled phalloidin and nuclei were stained with DAPI. Finally, one drop of ProGold Anti-Fade was added to each well just before a cover slip was applied and sealed down with fingernail polish. The slides were allowed to dry and confocal sections were images with an Olympus IX81 microscope with a 100X oil objective using SlideBook software from Intelligent Imaging Innovations, Inc, Denver, CO. Alternatively, J774 macrophages grown in sterile glass-bottom 96-well plates were incubated for 15 min with Alexa-labeled recombinant IpaD. Wells were washed three times with sterile PBS. A live cell imaging solution was added and live images collected 1 hour post-treatment with an Olympus IX-83 motorized microscope with a 20x objective using CellSense software from Olympus, Center Valley, PA. Phase contrast, differential interference contrast and appropriate excitation channels were collected.

Introduction of Recombinant IpaD into macrophages: Cells were grown in 96- and 6-well plates or in T-25, -75 or -150 according to the downstream technique desired. Recombinant IpaD purified as described above was concentrated with Amicon Ultra centrifugal filter units to a protein

concentration of approximately 10 mg/ml. Then, at least 30 min before incubation with the cells, an appropriate amount of IpaD was incubated with LDAO to a concentration of 0.1%. Protein was then added to cells in a serum-free media (either DMEM or RPMI) so that the final concentration of the protein was in the μM range and the final concentration of LDAO was 0.001%. Final concentration of LDAO at 0.001% was maintained in each well/flask by addition of an appropriate amount of 0.1% LDAO in PBS.

Cytotoxicity of macrophages: Cells were grown at a concentration of $2x10^4$ cells/well in a 96-well plate and treated with the appropriate amount of recombinant protein or at an MOI of 1:100 for infections with *Shigella*. The 96-well plate is then centrifuged at 250 x g for 4 min at room temperature. 50 μl of the supernatant were transferred to a flat-bottom non-coated 96-well plate. The LDH working solution is prepared by mixing 12 ml of the assay buffer with one vial of substrate mix of a CytoTox 96 non-radioactive cytotoxicity assay kit. The LDH working solution measures released lactate dehydrogenase in culture supernatants, which results in the conversion of a tetrazolium salt into a red formazan product. The amount of red color is proportional to the number of lysed cells. 50 μl of the working solution are mixed with supernatants in the 96-well plate, and incubated in an orbital shaker for 30 min at room temperature. 50 μl of stop solution (10% acetic acid) are added to each well. Any air bubbles are popped with a 10 μl pipette tip and absorbance read at 490 nm with a Spectramax plate reader. The percent of cytotoxicity was calculated as: 100 × [(experimental release − background release)/(total release − spontaneous release)]. In this formula, the background release represents the amount of LDH present in the supernatant of a vehicle control (cells exposed to 0.25% DMSO in caspase-inhibitor assays or 0.001% LDAO for purified protein experiments), the spontaneous release represents the amount

of LDH present in the supernatant of cells exposed to PBS and the total release is the amount of LDH by cell lysis with a Triton X-100 solution.

Caspase activity determination: Cells grown in a 96-well plate were incubated with 2.4 μM recombinant IpaD for 30 min at 37°C, 5% CO_2. The plate is then removed from the incubator and allowed to equilibrate to room temperature. Reconstituted Caspase-Glo reagents for caspases -2, -3, -8 and -9 were used. 100 μl of Caspase-Glo reagent were added to each well and incubated for 30 min. Luminescence was measured with a Spectramax plate reader, and corresponds to the activity of the caspase measured.

Cell death inhibition: J774 macrophages were treated with recombinant protein or Shigella strains as indicated above. Prior to treatment, the cells in a 96-well plate were incubated for 1 hour at 37°C, 5% CO2 with 50 μM of the caspase inhibitors Z-VAD-FMK (pan-caspase), Z-WEHD-FMK (caspase-1), Z-YVAD-FMK (caspase-1), Z-VDVAD-FMK (caspase-2), Z-DEVD-FMK (caspase-3), Z-IETD-FMK (caspase-8), and Z-LEHD-FMK (caspase-9 or -11). The effect of a caspase inhibitor on cytotoxicity was measured in relation to controls without it.

Caspase-3 activation: Macrophages were seeded at a concentration of 6 x 10^5 in a 6-well plate and incubated overnight to allow for attachment to the plate. Cells were then exposed to IpaD at times 15, 30, 60, 90 and 120 min. as described above. The cell supernatants were collected, and a solution of Accutase was added to the cell monolayer for detachment. After 10 min. at 37°C, the cells were recovered as a single cell suspension. The well was washed with PBS. The cell suspension and the PBS from the wash were pooled with the cell supernatants. Then, cells were centrifuged at 400 x g for 5 min. at room temperature. The cell pellet was resuspended in 200 μl of PBS and 1 μl of a 1 mM NucView 488 caspase-3 enzyme substrate in DMSO was added and cells were gently mixed. The cells were incubated for 15 min. at room temperature and promptly

put on ice. 300 µl of PBS were added to each tube and whole preparation transferred to a flow cytometry tube. The fluorescence was measured with a blue laser and a detector at 488 nm. Baseline fluorescence was measured in cells without staining.

Mitochondrial disruption: The mitochondrial membrane potential was measured with the cell-permeable dye JC-1, which emits fluorescence at 488 nm when soluble in the cytoplasm and at 568 nm when aggregated inside the mitochondrion. JC-1 working solution is made by adding 10 µl of the 100X JC-1 dye in DMSO into 1 ml of assay buffer (saline solution provided by the manufacturer). Cells were treated and collected as described for caspase-3 activation above. The cell pellet was resuspended in 500 µl of the JC-1 working solution and incubated for 15 min. at 37°C, 5% CO_2. Cells were centrifuged at 400 x g for 5 min and washed twice with PBS. Finally, cells were resuspended in 500 µl of PBS, immediately put on ice and transferred to a flow cytometry tube. The fluorescence was measured with a blue laser and a detector at 488 nm, and with a green-yellow laser and a detector at 568 nm. Baseline fluorescence was measured in cells without staining.

Annexin V/Propidium Iodide staining: Cells were treated and collected as described above. The cell pellet was washed with 1 ml of ice-cold PBS. Cells were resuspended in 100 µl of Annexin-binding buffer. To this volume, 5 µl of FITC Annexin V dye and 1 µl of 100 µg/ml PI working solution were added. Cells were incubated for 15 min at room temperature. After incubation, 400 µl of Annexin-binding buffer were added and cells were immediately placed on ice. Cell suspension was transferred to a flow cytometry tube and fluorescence measured with a blue laser and a detector at 488 nm, and a green-yellow laser and a detector at 568 nm. Baseline fluorescence was measured in cells without staining.

Flow cytometry: All flow cytometry was performed at the Kansas Vaccine Institute Immunology Core Laboratory (KVI-ICL). The instrument used for flow cytometry was a BD FACSAria Fusion setup with lasers at 405 (violet), 488 (blue), 561 (yellow-orange), and 640 (red) nm. These lasers are coupled to 11 different filters, which enables the use of several fluorophores in the same sample. BD FACSDiva Cytometer Setup and Tracking (CS&T) Research Beads are used for automated setup of the instrument. Voltages for each detector are setup using an unstained control, which represents the background fluorescence of the sample. All samples are gated for specific populations according to the manufacturers' specifications for each kit.

CHAPTER III: Analysis of the Role of IpaD on Cell Death in Macrophages

Introduction

Shigella's ability to cause disease depends on the presence of the virulence plasmid, as evidenced by early studies with *Shigella* strains that had lost the virulence plasmid[97] or those with large deleted regions in the plasmid[98]. Further investigation demonstrated that one of the characteristics of *Shigella* losing its virulence plasmid is the inability to induce cell death. In a rabbit ligated ileal loop model, animals infected with wild-type *Shigella* had intestinal lymphoid follicles with apoptotic macrophages, T and B cells, whereas no apoptosis was detected for rabbits challenged with a plasmid-cured *Shigella* strain[58].

The normal state of a healthy cell is preserved through homeostatic cell processes including the balance between their proliferation and cell death depending on the requirements of the tissue in which they reside and the stimuli present in their environment. There are insults that a cell or population of cells can receive that trigger morphological, functional and biochemical changes that are irreversible and hamper cell viability. Cell death can occur as the result of numerous insults such as UV and ionizing radiation, toxins, microbial and viral infections, or nutrient withdrawal. Cell death can occur through several mechanisms that are either unregulated or regulated. Unregulated cell death is called necrosis, and is a passive catastrophic type of death that arises without energy (ATP) consumption. Necrotic cells swell and their plasma membrane ruptures, leaking their contents onto the extracellular environment. This results in a high degree of inflammation and further damage to neighboring cells[99]. Regulated types of cell death that have been described are apoptosis, necroptosis, pyroptosis, and autophagy[100].

Apoptosis (a term meaning *shedding of leaves* in Greek) is a type of programmed cell death that aids in the healthy turnover of cells in tissue, but can also be the result of pathological stimuli[101]. If cells cannot repair the damage (for example, using anti-apoptotic cytokine IL-2 or DNA repair mechanisms), they reach a point of no return where they are now committed to die[102]. Morphological changes in apoptotic cells are well conserved independent of the triggering stimuli, and include cell shrinking, formation of membrane blebs, chromatin condensation (karyopyknosis), fragmentation of nuclei (karyorrhexis), and separation of cell fragments into apoptotic bodies[101]. The main feature of apoptosis is that it is a non-inflammatory pathway because the cellular contents are enclosed in an intact plasma membrane (apoptotic bodies), such that no damage is caused to neighboring cells. Commonly described as programmed cell death, it is a tightly regulated process orchestrated by caspases, a family of cysteine-dependent aspartate-directed proteases[103]. Caspases cleave cellular targets as a cascade of cell degradation that results in the complete disassembly of chromatin and irreversible changes to organelles like mitochondria and the endoplasmic reticulum[104,105]. The role of mitochondria in apoptosis has been well studied. Pro-apoptotic proteins can disrupt the outer mitochondrial membrane, allowing the release of Cytochrome C into the cytoplasm. This is received by the cell as a point of no return signal. Therefore, the study of mitochondrial function in cell death analysis is necessary[102,106,107].

In 1992, Zychlinsky et al. described for the first time that *Shigella* could kill macrophages and that this phenomenon was tied to its virulence plasmid[108]. Additional studies described this type of death as a new mechanism different from apoptosis, in which high levels of IL-1β and IL-18 are elicited by activation of caspase-1[62]. This inflammatory type of cell death is now called pyroptosis and has since been found to occur in infections by other pathogens harboring a T3SS[63,109]. Although the translocator protein IpaB is able to directly bind caspase-1 *in vitro*[110], other reports

have found that this is not sufficient for pyroptosis. Experiments with methyl-beta-cyclodextrin, a cholesterol-sequestering compound, showed that if phagocytosis and phagosomal escape were allowed to progress normally, secretion of IpaB was not impaired by cholesterol sequestering but macrophage cell death was[111]. IpaB was also found to spontaneously form potassium channels, and it is this potassium flux that triggers caspase-1 activation, possibly through IPAF (NLRC4) inflammasome activation[64]. These studies show the association of IpaB with the host membrane and the vacuolar damage triggered are necessary for the induction of pyroptosis. Also, pyroptosis caused by the activation of caspase-11 non-canonical inflammasomes in response to intracellular LPS has been studied in several gram-negative pathogens including *Shigella*[65,112].

There is evidence of other types of macrophage cell death triggered by *Shigella*, however, these have been studied less extensively. The cell line U937 has been used to study the effect of *Shigella* in human cells. U937 is a human monocyte cell line that can be differentiated into macrophages *in vitro* by different stimuli[113]. Nonaka et al. used interferon gamma (IFN-γ) and retinoic acid (RA) and found that IFN-differentiated macrophages exhibited some of the classical signs of apoptosis such as DNA fragmentation and cleavage of a caspase substrate upon *Shigella* infection[114]. The RA differentiated macrophages in turn died by oncosis, another type of cell death that shows cell swelling, and some authors have concurred that this is a type of necrosis[115,116]. Necrotic cell death through an inflammasome pathway was studied later[60]. Furthermore, Hilbi et al. concluded that only caspase-1 was necessary for *Shigella*-mediated macrophage cell death, however, their experiments show that casp1 -/- macrophages still show a cytotoxic response of approximately 25%[110]. No recent studies have been dedicated at discerning the mechanisms or contributing factors to the alternative types of cell death observed during *Shigella* infection.

The ability of *Shigella* to cause apoptosis was revisited when Nothelfer et al. studied the effect of *Shigella* infection of B lymphocytes. They found that B cell death could be elicited by *Shigella* in a T3SS-dependent manner. They further concluded that the virulence factor IpaD behaved like a TLR2 agonist and in this role could contribute to cell death. Their experiments show purified IpaD could be used as a contributing factor to apoptosis in B lymphocytes only when coupled with a T3SA$^-$ *Shigella* strain[96]. The lack of evidence of a particular factor causing apoptosis in macrophages, and the potential of IpaD to cause this type of cell death opened the possibility for the study of IpaD as an apoptotic factor in macrophages.

Results

The studies showing apoptosis could be caused by *Shigella* upon infection were limited but other studies provided information about *Shigella* killing through more than one pathway upon further examining their experimental sets[59,110]. In order to determine if apoptosis could indeed be elicited by a wild-type *Shigella* strain in an experimental model, we planned to infect cultured macrophages with *S. flexneri* serotype 2a strain 2457T, which we have used extensively in previous studies. First, we looked for an *in vitro* model that was robust and well-cited for the study of macrophage biology, especially in the setting of infection. The earliest account of macrophages dying due to *Shigella* infection is the 1987 study by Clerc, et al. in which they observed that a virulent *S. flexneri* strain was able to kill macrophages of the J774 cell line and that this correlated with the intracellular presence of the bacterium and a strain harboring a complete virulence plasmid[117]. In the following years, J774 cells were utilized to further study this phenomenon[118–122]. In one study, the invasiveness of wild-type *S. flexneri* strain YSH6000 was evaluated in cell lines J774, RAW264.7 and THP-1, and the bacteria were found to be most efficient at invading

J774 cells[123]. This cell line has also been widely used as a model in several studies in other aspects of *Shigella* pathogenesis as well as that of other bacteria with a T3SS[124–127].

We infected macrophages of the J774 cell line with the wild-type *S. flexneri* strain, at a multiplicity of infection (MOI) of 1:100. The cell death caused in an *in vitro* setting can be measured by the release of LDH into the supernatant of cells grown in a cell culture plate well. *S. flexneri* was able to kill 78% of the total population (first bar, **Fig. 2**) after 2 hours of infection.

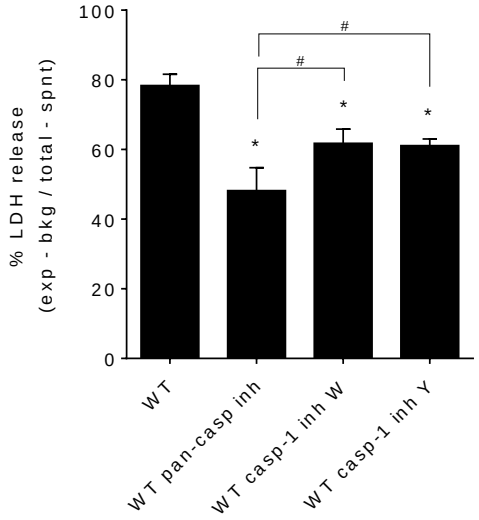

Fig. 2 Cytotoxicity elicited in J774 macrophages by a wild-type *S. flexneri* strain. Bacterial infection of macrophages *in vitro* shows that most of the cell population has died at 2 hours post-infection. The cytotoxicity in the presence of caspase inhibitors was also assessed (50 μM of pan-caspase inhibitor, Z-VAD-FMK; casp-1 inhibitor W, Z-WEHD-FMK; casp-1 inhibitor Y, Z-YVAD-FMK. One-way ANOVA analysis ($p<0.05$). *treated vs WT, #caspase-1 vs pan-caspase inhibitor treatment.

In order to investigate apoptotic responses triggered by *Shigella* infection, the cytotoxicity in the presence of caspase inhibitors was also assessed. The inhibitor Z-VAD-FMK is known to inhibit all caspases as it can bind irreversibly in their active site[128]. After pre-incubation with this pan-caspase inhibitor, J774 macrophages were infected with the wild-type *S. flexneri* strain for 2 hours. Inhibition of caspases results in a decrease in cell death of 40% (**Fig. 2**). Since there is evidence that caspase-1 is an important factor in macrophage death by pyroptosis, we pre-incubated cells

with caspase-1 inhibitor Z-WEHD-FMK and subsequently infected the cells with wild-type bacteria. The caspase-1 inhibitor decreases killing by only 20%. A similar level of reduction was seen by pre-incubation with Z-YVAD-FMK, another caspase-1 inhibitor (**Fig. 2**). A reduction in cell death by a caspase-1 inhibitor is expected as per previous observations by other authors in which caspase-1 is necessary for macrophage cell death, that is, by a pyroptosis pathway, however, the fact that inhibition of caspase-1 is less efficient at reducing cell death than pan-caspase inhibition might indicate that macrophage death is, at least in part, caused by other caspases.

To assess the role of IpaD in the cytotoxicity seen with wild-type *Shigella* infections, we used a model in which we can manipulate the presence or absence of functional IpaD in the bacterium. *S. flexneri* strains carrying null mutations have been widely used in the literature. An *ipaD* null strain (SF622)[87] is able to grow in both solid and liquid media, however, due to the structural role of IpaD in the T3SA, it is avirulent but shows uncontrolled secretion. When complemented with a plasmid for expression of IpaD ($IpaD^+$ strain), the defect is rescued and the strain behaves like the wild-type strain with regard to secretion control and virulence[88,89]. Indeed, we were able to emulate the cytotoxicity profile of the wild-type strain with the $IpaD^+$ strain (**Fig. 3**). Pre-incubation with the pan-caspase inhibitor also reduced the cytotoxicity of the strain. As mentioned before, it has also been reported that caspase-11 is needed for pyroptosis by *Shigella* infection, due to intracellular LPS recognition within the macrophage[65]. In order to eliminate both sources of pyroptosis (caspases -1 and -11), we pre-incubated cells with both Z-YVAD-FMK and Z-LEHD-FMK (an inhibitor of caspases -9 and -11). The $IpaD^+$ strain showed reduced cytotoxicity in this sample, however, the difference was not significant. This might due to elevated levels of IpaD due to plasmid expression or an effect of two inhibitors, instead of one, present in the sample.

Macrophages were then infected with three strains encoding IpaD proteins with deletions within the N-terminal domain: IpaD$^{\Delta 41\text{-}80}$, IpaD$^{\Delta 81\text{-}120}$, and IpaD$^{\Delta 111\text{-}120}$. These strains had previously been characterized by our group for invasion of epithelial cells and all retained 100% invasiveness when compared to the IpaD^{+} strain. *S. flexneri* strains IpaD$^{\Delta 81\text{-}120}$ and IpaD$^{\Delta 111\text{-}120}$ did not show a major defect in their killing potential, as their cytotoxicity did not differ significantly from that of IpaD^{+}. Strain IpaD$^{\Delta 41\text{-}80}$ is the only one to show a significant reduction in cell death when compared to IpaD^{+} (**Fig. 3**). As described above, when cells are pre-incubated with a pan-caspase inhibitor, infection with the IpaD^{+} strain results in diminished cytotoxicity vs. the cytotoxicity this strain causes with no inhibitor present. The same inhibitory effect is seen for the cytotoxicity caused by any of the mutant strains. However, only the cytotoxicity of the IpaD$^{\Delta 41\text{-}80}$ strain is greatly reduced by pan-caspase inhibition (83% reduction). Pre-incubation of cells with caspases -1 and -11 inhibitors also greatly reduced the cytotoxicity of IpaD$^{\Delta 41\text{-}80}$ (79% reduction). The cytotoxicity caused by IpaD$^{\Delta 41\text{-}80}$ was thus greatly reduced from that of IpaD^{+} in similar inhibitory conditions. These results indicate that by removing the effect of caspases driving pyroptosis (caspases -1 and -11), IpaD$^{\Delta 41\text{-}80}$ is nearly unable to cause cytotoxicity (**Fig. 3**).

The effect seen for IpaD$^{\Delta 41\text{-}80}$ could be due to several factors. A structural defect caused by the loss of a large region (**Fig. 4**) could cause the protein to be unable to fully function as a part of the T3SA, however, this is unlikely as it the strain is able to invade epithelial cells correctly. Defects in the ability of the strain to pierce the membrane (i.e. form translocon pores) would render IpaD unable to reach the macrophage cytoplasm, where *Shigella* can modulate the cell survival. The ability to form translocons in the membrane can be assessed by a contact-mediated hemolysis assay. A *Shigella* strain is incubated with sheep's blood for 1 hour, in which the outer membrane of the red blood cells is pierced by a functional translocon. Cells are then extruded with cold PBS

and hemoglobin released. The percent of hemoglobin in the supernatant is proportional to the hemolytic activity of the strain. Although IpaD$^{\Delta 41\text{-}80}$ had been characterized before by our group[88], it was assessed again to establish the phenotype was currently the same. The hemolytic activity of IpaD$^{\Delta 41\text{-}80}$ is not significantly different to that of IpaD^{+} (**Fig. 5**).

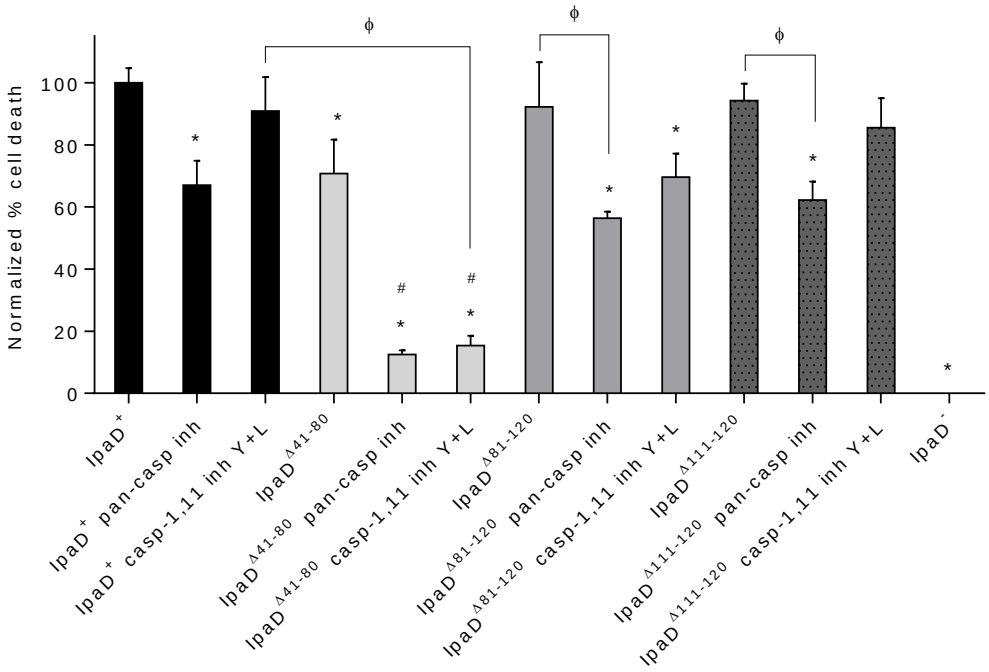

Fig. 3. Cytotoxicity profiles of *S. flexneri* strains with N-terminal deletions. Macrophages were infected at an MOI of 1:100 for 2 hours with ipaD null strains carrying a plasmid for expression of wild-type IpaD (IpaD^{+}), IpaD deleted in amino acids 41-80 (IpaD$^{\Delta 41\text{-}80}$), IpaD deleted in amino acids 81-120 (IpaD$^{\Delta 81\text{-}120}$), and IpaD deleted in amino acids 111-120 (IpaD$^{\Delta 111\text{-}120}$). All strains were then used in macrophages pre-treated with caspase inhibitors as described in Fig. 2. Data was normalized using IpaD^{+} as 100%. One-way ANOVA analysis ($p<0.05$). *vs IpaD^{+} with no inhibitors, #vs IpaD$^{\Delta 41\text{-}80}$, $^{\phi}$vs connected bar.

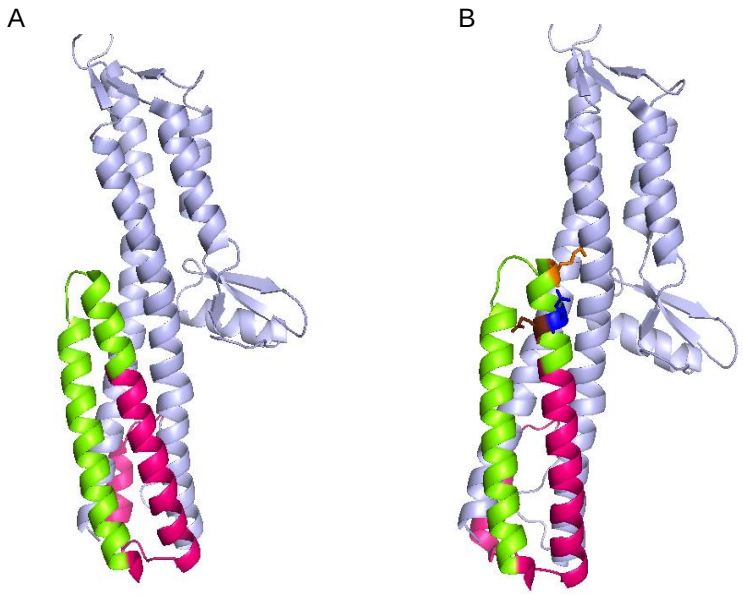

Fig. 4. 3D structure of IpaD (PDB 2J0O). The crystal structure of IpaD has been solved from amino acids 39-322. IpaD is a hydrophilic protein with a highly α-helical structure. It has a hairpin structure in its N-terminal domain, which spans amino acids 1-120 (shown here in red). The region depicted in green corresponds to amino acids 41-80, which were found to be important for cytotoxicity in a complemented strain. A) IpaD$^{\Delta 41\text{-}80}$ would lack the aminoacids highlighted in green. B) Aminoacids highlighted are K72 (orange), E76 (blue), and E77 (brown).

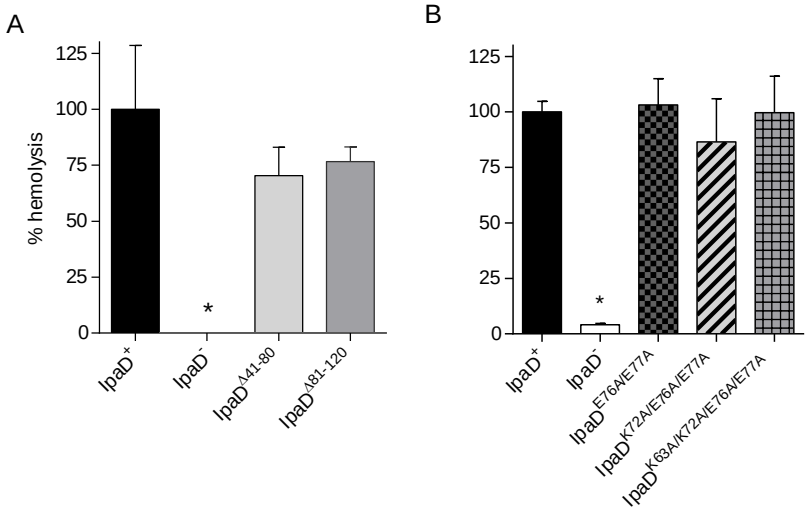

Fig. 5. Hemolysis of *S. flexneri* strains. The ability of a strain to assemble a functional translocon is assessed through its ability to pierce the membrane of RBCs in contact-mediated hemolysis assays. The strains with a functional T3SA will exhibit the same degree of hemolytic activity than IpaD^{+}. An IpaD^{-} strain exhibits no hemolytic activity. A) Hemolytic activity of N-terminal deletion strains IpaD$^{\Delta 41\text{-}80}$ and IpaD$^{\Delta 81\text{-}120}$. B) Hemolytic activity of strains with point mutations in IpaD. No significant differences were found for the hemolysis caused by any of the mutant complemented strains. Data was normalized using IpaD^{+} as 100%. One-way ANOVA analysis ($p<0.05$). *vs IpaD^{+}.

A reduced ability to escape the phagosome, independent of a strain's ability to form functional translocons in the membrane, could also lead to reduced cytotoxicity as bacteria would be unable to access the cytosol. The phagosomal escape ability was assessed with a modified gentamicin assay in which chloroquine is introduced. Chloroquine is a DNA intercalator that accumulates in lysosomes and is a potent antimalarial drug. In our study, we used chloroquine with *S. flexneri* infected macrophages because the chloroquine should accumulate in the phagosome and kill all bacteria unable to escape into the cytoplasm. Cytoplasmic bacteria are quantified by the differential of bacteria from cells incubated with and without chloroquine. IpaD$^{\Delta 41\text{-}80}$ is equally able to escape the phagosome as the IpaD^{+} strain since the number of cytoplasmic bacteria recovered from macrophages was comparable in each case (**Fig. 6**).

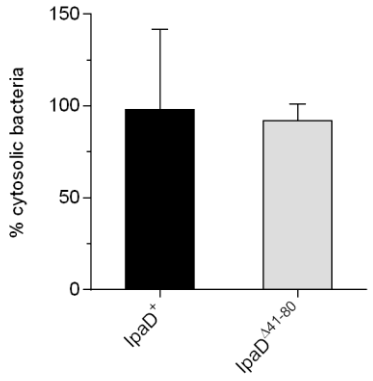

Fig. 6. Phagosomal escape of *S. flexneri* strain IpaD$^{\Delta 41\text{-}80}$. The ability of a strain to escape the phagosome after infection of a macrophage can be investigated with a modified gentamicin protection assay. Cells are incubated in the absence or the presence of chloroquine, a compound that kills bacteria trapped in the phagosome. The percent of cytosolic bacteria represents the amount of bacteria that are unaffected by the addition of chloroquine ((CFU in gentamicin plus chloroquine/CFU in gentamicin) x 100). The values were not found to be significantly different. Significance was calculated with an unpaired t-test ($p<0.05$).

Thus, the ability of IpaD$^{\Delta 41\text{-}80}$ to most efficiently kill the macrophage is impaired for reasons beyond the fitness of its T3SA. In an attempt to investigate the extent of what this region contributes to *Shigella* cytotoxicity, we performed cytotoxicity assays with mutants already available in our stocks. Three strains were identified, with point mutations in the corresponding region: E76A/E77A, K72A/E76A/E77A, and K63A/K72A/E76A/E77A. All these strains show a similar profile of overnight secretion relative to IpaD^{+}, as analyzed by precipitation of culture supernatants (**Fig. 7**). Similarly, the induction of secretion by Congo red was unchanged, except for the mutant IpaD$^{K63A/K72A/E76A/E77A}$ which exhibits slightly higher IpaD secretion (**Fig. 7**). These profiles indicate that the mutations do not impair the function of IpaD in secretion control. The cytotoxicity caused to macrophages by these strains was measured using the LDH release assay. Only IpaD$^{K72A/E76A/E77A}$ showed a significant decrease in cytotoxicity when compared to IpaD^{+} (**Fig. 8**). Furthermore, none of these mutant strains have a defect in hemolytic activity (**Fig. 5**). The IpaD crystal structure highlighting the N-terminal region of amino acids 41-80 and the residues K72, E76 and E77 is depicted in **Fig. 4**.

As can be seen in the 3D structure, the residues mutated in strain IpaD$^{K72A/E76A/E77A}$ are surface exposed and located at the top of the hairpin formed by the N-terminal domain of IpaD. It is interesting that the strain with the additional mutation in K63 is able to restore the IpaD cytotoxicity. We are unsure why this difference is observed but we plan to perform additional experiments in the future that may allow us to discern the difference in these mutants. A mutation in only K72 and a mutant in Q165, a residue in the coiled-coil region likely to interact with K72, should be considered as part of these future experiments.

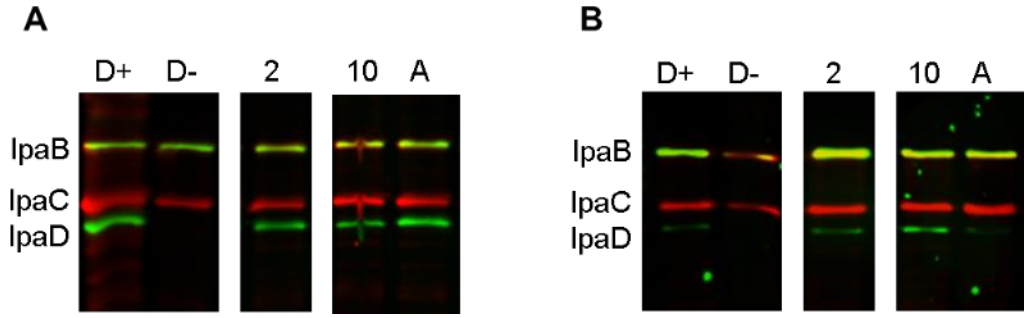

Fig. 7. Secretion profiles of *S. flexneri* strains. The secretion profiles of strains with N-terminal point mutations were assessed for overnight secretion of *ipa* effectors as well as secretion upon stimuli. Strains are labeled as follows: D+ is IpaD^{+}, D- is IpaD^{-}, 2 is IpaD$^{K72A/E76A/E77A}$, 10 is IpaD$^{K63A/K72A/E76A/E77A}$, and A is IpaD$^{E76A/E77A}$. A) Overnight secretion in a culture is evaluated by precipitating the supernatant with TCA, resuspension and immunoblotting. All complemented strains show comparable amounts of IpaB, IpaC and IpaD secreted onto the extracellular environment. B) Immunoblot of proteins secreted after addition of Congo red, an anionic dye used as an inducer of the T3SS. IpaD is secreted in similar amounts upon induction in complemented strains, except for IpaD$^{K63A/K72A/E76A/E77A}$ that was found to secrete higher levels of IpaD.

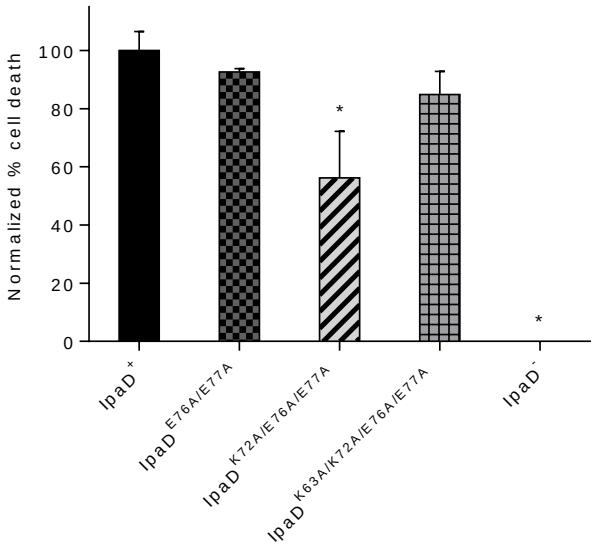

Fig. 8. Cytotoxicity profiles of *S. flexneri* strains with point mutations. The LDH release of macrophages caused by infection with point mutant strains was measured at 2 hours post-infection. Strain IpaD^{-} is unable to cause cytotoxicity. Mutants IpaD$^{E76A/E77A}$ and IpaD$^{K63A/K72A/E76A/E77A}$ show no significant difference in their cytotoxic profile, whereas mutant IpaD$^{K72A/E76A/E77A}$ shows reduced cytotoxicity. Data was normalized using IpaD^{+} as 100%. One-way ANOVA analysis ($p<0.05$). *vs IpaD^{+}.

Cytokine cleavage and secretion by macrophages is one of the hallmark signs that the process of pyroptosis has started and this has been reported for macrophages infected with *Shigella*[111]. Therefore, we analyzed the cytokine secretion profiles of J774 macrophages infected with the mutant identified as defective in cytotoxic potential (IpaD$^{\Delta 41\text{-}80}$). IL-1β secretion of cells infected with IpaD^{+} or IpaD$^{\Delta 41\text{-}80}$ is comparable. IpaD^{-} secreted minimal levels of IL-1β. When macrophages are pre-incubated with a pan-caspase inhibitor or with caspases -1 and -11 inhibitors, IL-1β secretion triggered by IpaD^{+} is reduced 4-fold. The same pattern is seen in infections with IpaD$^{\Delta 41\text{-}80}$ (**Fig. 9**). Therefore, macrophages infected with IpaD$^{\Delta 41\text{-}80}$ have no defect in IL-1β secretion. Furthermore, these results serve as evidence that the caspases -1 and -11 inhibitors used for the study are able to block a pyroptosis process. IL-18 secretion, which is an event downstream of IL-1β secretion, has previously been indicated to be another mediator of inflammation caused by *Shigella* infection[129]. The profiles of IL-18 secretion were all similar in the infection conditions used to monitor the differences in IL-1β secretion and there was no effect detected by caspase inhibition. Thus, the level of IL-18 secretion was the same as the basal level J774 macrophages incubated only with media showed (**Fig. 9**).

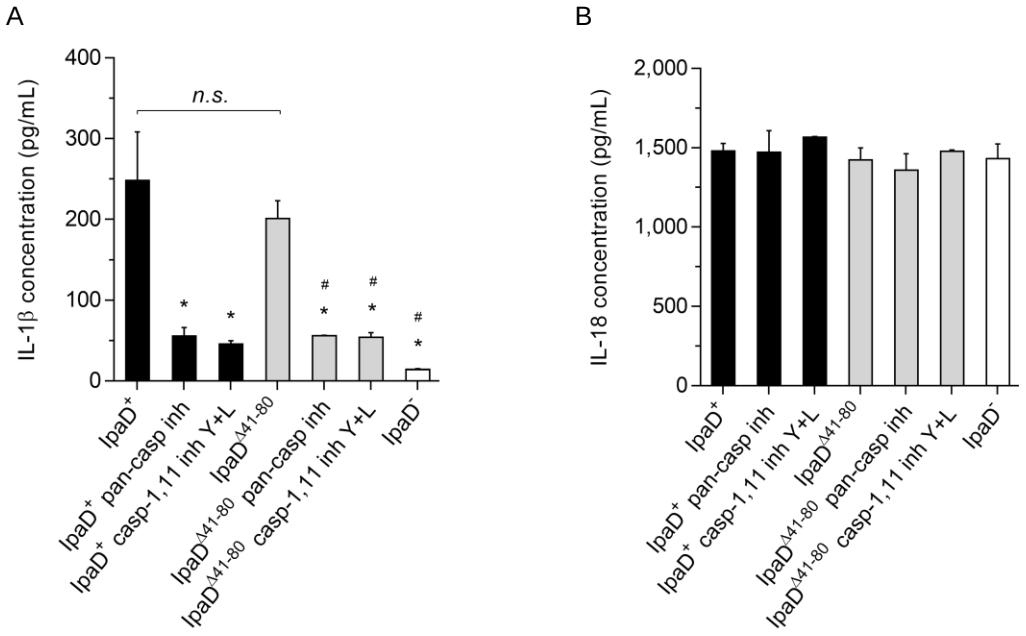

Fig. 9. Cytokine profiles for macrophages infected with *S. flexneri* strains. The inflammation seen with pyroptosis is a result of inflammatory cytokines that are released upon caspases -1 or -11 activation. The amount of cytokine secretion can be quantified from supernatants of macrophages infected with bacterial strains. A) The secretion profile for cytokine IL-1β upon infection of macrophages with IpaD^{+} or IpaD$^{\Delta 41\text{-}80}$. Caspase inhibition is able to greatly reduce the amount of IL-1β secreted. B) Cytokine IL-18 secretion levels were measured in supernatants of cells infected with IpaD^{+} or IpaD$^{\Delta 41\text{-}80}$. IL-18 secreted by infected macrophages are all comparable. Significance was calculated with a one-way ANOVA analysis ($p<0.05$) *vs IpaD^{+}, #vs deletion mutant, n.s. not significant.

One of the main obstacles to working with mutant strains is having to maintain ideal conditions of inhibition by extraneous factors that are also contributing to macrophage cell death caused by *Shigella*. With purified protein, we were able to emulate the cell death caused by the infection using purified recombinant IpaD. In this way, we expected a robust model for the analysis of the mechanism behind the role of IpaD in macrophage cell death. Unfortunately, IpaD is highly hydrophilic and simply exposing a macrophage population to IpaD *in vitro* did not result in the internalization of the protein, and thus no effect was seen (**Fig. 10**). A report by Taylor and Fernandez-Patron showed that a mild detergent could be used to transduce proteins into cells, without affecting viability[130]. We examined the effect of LDAO, the zwitterionic detergent used

to maintain recombinant IpaB in a soluble state on IpaD entry into J774 cells. We found that the morphology of cells exposed to LDAO in small concentrations remains unchanged (**Fig. 10**). When macrophages were incubated with IpaD in the presence of LDAO, the protein was internalized within 15 minutes (the number of cells with internalized IpaD was 97.9% ± 2.3%). The morphology of the cells changes at 1 hour post-exposure, and cell shrinking, membrane blebbing and the presence of apoptotic bodies is seen (**Fig. 10**).

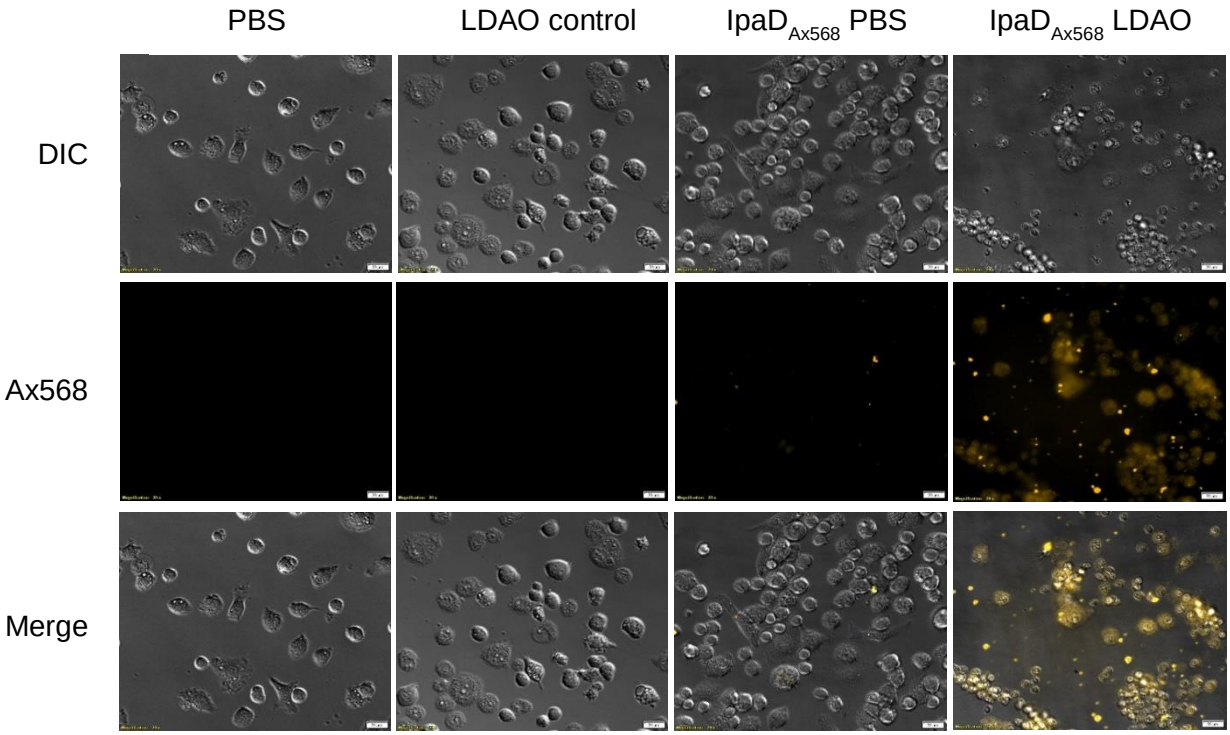

Fig. 10. IpaD is internalized in the presence of LDAO. The introduction of IpaD into macrophages is necessary for a model that emulates the effect of IpaD by *Shigella* infection, as cytoplasmic bacteria will kill macrophages. By exposing macrophages to LDAO, Alexa-568 labeled IpaD in PBS or Alexa-568 labeled IpaD with LDAO, we were able to analyze the effect of protein transduction with a mild detergent. Cells were incubated with treatment for 15 min and then washed extensively. Live cells were imaged 1 h after treatment. IpaD delivered in PBS was unable to enter cells as shown by a low intracellular signal. Cells exposed to IpaD with 0.001% LDAO show internalization of recombinant IpaD.

In this model, as implied by the changes in cell morphology, recombinant IpaD is able to cause cell death of a macrophage population *in vitro*. In ranges from 0.2 to 2.4 μM IpaD causes cell death in a dose-dependent manner (**Fig. 11**). Another macrophage cell line, RAW264.7 was killed in a similar way as the J774 macrophages. In primary cells such as bone marrow-derived macrophages, IpaD displays somewhat less cytotoxicity although the effect is still dose-dependent. In a human monocyte cell line, if this population is differentiated onto macrophages, IpaD is also cytotoxic. The effect seen is specific for recombinant IpaD since a negative control was assessed by introducing recombinant IpgC (with no effector function) in an equal amount of LDAO. This negative control showed no cytotoxicity (**Fig. 11**). The model developed is thus robust and can be used to emulate the death caused by IpaD. This model allowed us to examine the mechanistic events leading to the cell death.

The N-terminal domain of IpaD (**Fig. 4**) is known to fold independent of the rest of the protein[131]. Thought to have a self-chaperoning effect, a conserved structure is found in SipD from *Salmonella* spp. and BipD from *Burkholderia pseudomallei*, however, the tip proteins LcrV from *Yersinia* spp. and PcrV from *Pseudomonas aeruginosa* do not contain this domain and in turn associate with an independent chaperone prior to their secretion[94,132]. Due to our observations with mutant strains, we hypothesized that a protein with this N-terminal domain may behave like IpaD in terms of cytotoxicity, and a protein lacking the domain would not be able to cause macrophage death. In line with this, SipD in LDAO was found to cause cytotoxicity in a dose-dependent manner. Meanwhile, LcrV in LDAO was unable to cause cell death (**Fig. 11**). This strengthened our hypothesis that the N-terminal domain of IpaD was involved in the process of macrophage death.

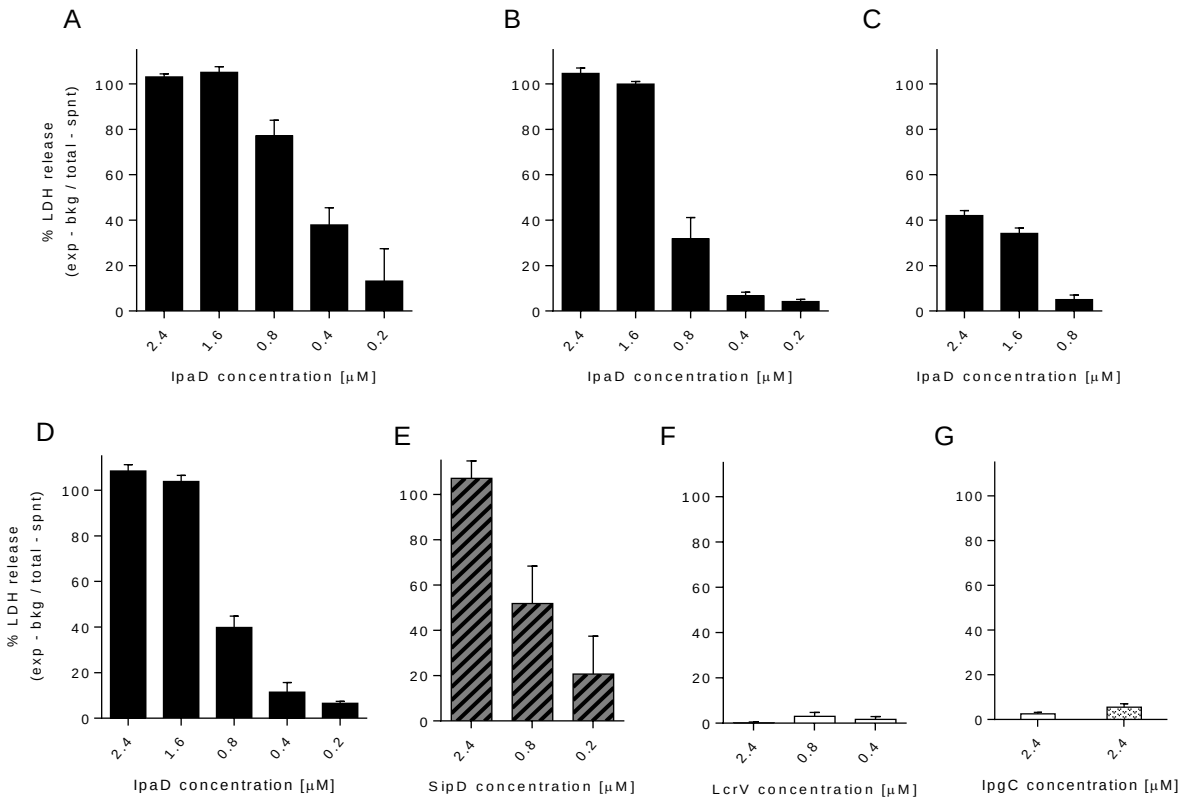

Fig. 11. Cytotoxicity profiles of recombinant proteins. The cytotoxicity in a model of recombinant IpaD was analyzed. The LDH release caused by incubation of different macrophage cell populations for 2 hours indicates that IpaD is able to cause cell death *in vitro*. A) J774 cell line. B) RAW264.7 cell line. C) Bone-marrow derived macrophages (primary cells). D) Differentiated U937 cell line. The effect of the N-terminal region of IpaD was compared to proteins with or without this domain. E) SipD in LDAO into J774 cells. F) LcrV in LDAO into J774 cells. G) A negative control with IpgC in LDAO into J774 cells.

Our experiments with *S. flexneri* strains showed that cytotoxicity in macrophages was caused by alternative caspase(s) other than caspases -1 and -11. Also, the morphology observed following the introduction of IpaD to macrophages was consistent with phenotypes of apoptotic cells. With our observations that mutant strains in IpaD are defective in cell death, we assessed if recombinant IpaD could activate caspases commonly found in apoptotic pathways[133]. With the use of peptides coupled to luciferin, caspase activity was assessed. If a certain caspase is activated, it will cleave the peptide in a specific manner and luminescence is detected. After 30 minutes of incubation with

either LDAO or IpaD in LDAO, activation of caspases was detected for caspases -2, -3, -8 and -9 (**Fig. 12**). Caspases -2, -8 and -9 are initiator caspases, meaning that they are able to start the cascade of substrate cleavage seen in apoptosis. Caspase-3 activity was also found to be significantly different than its control, however, the fold-increase was lower than that of initiator caspases (**Fig. 12**). This result would be expected if at the time of analysis the apoptotic cascade was in its initial stages. When caspase activation is inhibited by pre-incubating the macrophage population *in vitro* with caspase inhibitors, we observe that the pan-caspase inhibitor is the most efficient at inhibiting cell death. The results seen in **Fig. 12** correspond to macrophages pre-incubated for 1 hour with a specific caspase inhibitor, followed by incubation with IpaD for 2 hours. All caspase inhibitors were found to inhibit cell death to different extents. Strikingly, the caspase-3 inhibitor was able to inhibit cell death by 50%. An explanation of this result is that although the different initiator caspase and pan-caspase inhibitors were more efficient at inhibiting cell death, their effect was not total. Incubation of macrophages with IpaD for 2 hours gives enough time for the non-inhibited activity of initiator caspases to trigger activation of caspase-3. Then, a caspase-3 inhibitor would further inhibit whatever amount of cell death could be caused by caspase-3, resulting in a lower and perhaps inefficient inhibition of cell death. However, the observation that pre-incubation with these peptides is unable to totally inhibit cell death may indicate that an additional mechanism is responsible for the cell death caused by recombinant IpaD. None of our results point to what this additional cause would be, or if it actually exists.

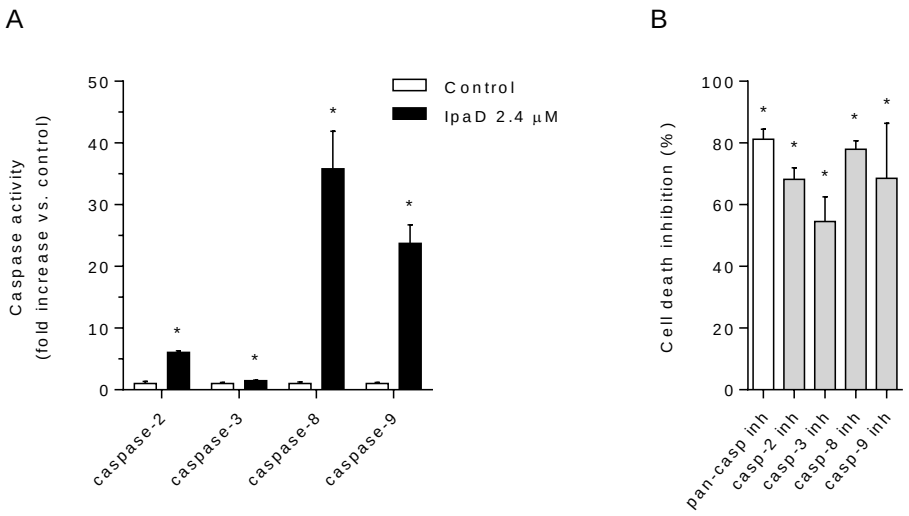

Fig. 12. Caspase activation after IpaD exposure and inhibition of death. The role of caspases in the macrophage death seen after exposure to IpaD was evaluated with caspase-specific peptides that can assess activity or, if modified, can inhibit them. A) Activity of apoptotic caspases was analyzed with luminescent substrates and luminescence captured as a measure of specific activity. B) The pre-incubation of J774 macrophages with pan-caspase inhibitor Z-VAD-FMK, caspase-specific inhibitors (caspase-2, Z-VDVAD-FMK; caspase-3, Z-DEVD-FMK; caspase-8, Z-IETD-FMK; caspase-9, Z-LEHD-FMK) or DMSO as a vehicle control and subsequent incubation with 2.4 µM IpaD results in inhibited cell death.

Following initiator caspase activation, the ensuing cascade within the cell committed to die would include cleavage and resulting activation of effector caspases. Of the initiator caspases seen as activated, all would be able to cleave and activate caspase-3. After 30 minutes of incubation with IpaD, a modest increase in caspase-3 activity was observed. As cell death progresses, caspase-3 activity would increase at the later time points. We assessed the activity of caspase-3 at 5, 15, 30, 60 and 120 minutes with a fluorescent substrate. The NucView dye is cell-permeable and accumulates inside the cytoplasm. If caspase-3 is active in the cytoplasm, it will cleave at the peptide region of the dye and release a DNA-binding dye that migrates to the nuclei where upon DNA binding will fluoresce. Our experiments indicate that caspase-3 is inactive up to 30 minutes, which is consistent with our luminescent substrate results (**Fig. 13**), however, at 1 hour after the

addition of IpaD, 40% of the macrophage population shows fluorescence, indicating increased activity of caspase-3.

At 120 minutes after IpaD addition, however, the population seems to have lost the fluorescence and a double peak is seen in the negative portion (**Fig. 13**). This phenomenon could be due to some of the population localizing outside the gate used in the cytometer setup method, as cells would be expected to be smaller in size if they have shrunken due to apoptosis. Another explanation is that the cells with activated caspase-3 at 1 hour are now dead or lysed and the population seen at 2 hours is enriched in the 60% of cells that did not have active caspase-3. Furthermore, this DNA-binding dye could show reduced fluorescence upon karyolysis, although this has not been reported thus far in published studies that used NucView.

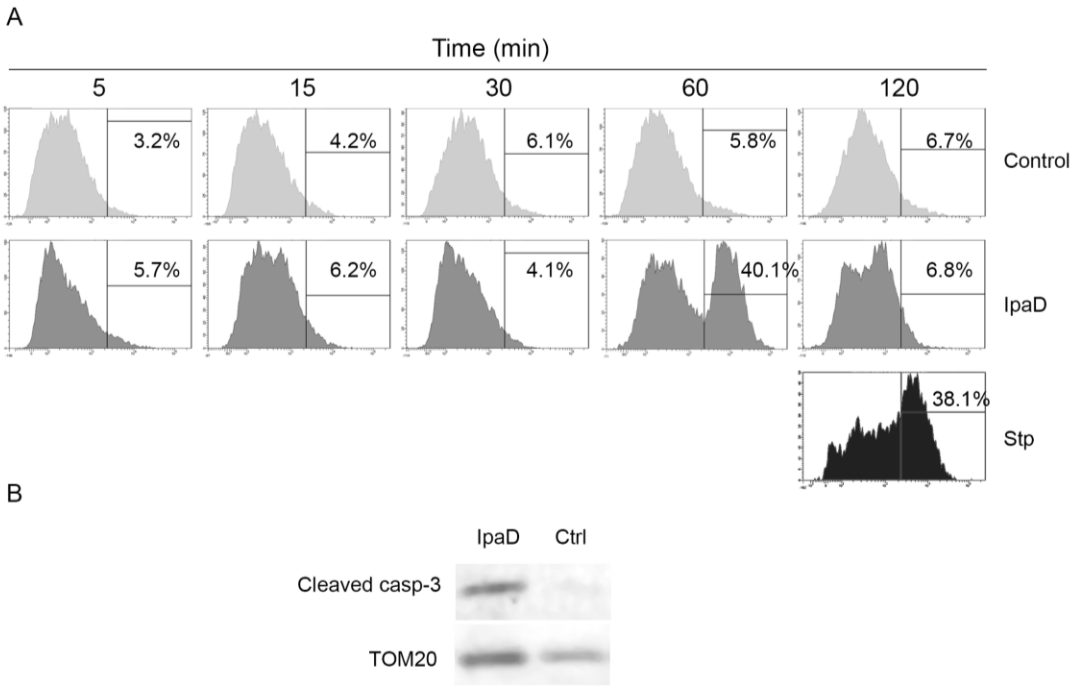

Fig. 13. Activation of caspase-3 in macrophages upon exposure to IpaD. The activity of effector caspase-3 was assessed at different time points. A) A fluorescent dye was used to analyze the activity of caspase-3 by flow cytometry. Staurosporine, a known apoptotic stimulant, was used as a positive control of caspase-3 activity. B) Immunoblot of lysates collected at 1 hour of macrophage incubation with IpaD were probed with an active caspase-3 antibody. TOM20, a mitochondrial protein was used as a loading control.

The activation of caspase-3 after 1 hour incubation with IpaD was confirmed by immunoblot with an antibody that only recognizes the cleaved variant of the caspase (**Fig. 13**).

The observation of active caspase-3 at 1 hour after the addition of IpaD to the macrophages would result in a certain cell population undergoing apoptosis. Annexin V is a fluorescent dye that attaches to the phosphatidylserine (PS) of the cell membrane. In healthy cells, PS is located toward the cytoplasm and Annexin V cannot bind to it as it is not cell-permeable. The externalization of PS is one of the events seen in apoptotic cells. Alternatively, if cells are undergoing necrosis, they will have lost cell membrane integrity totally and will be stained by propidium iodide (PI). Cells incubated with IpaD for 1 hour show a macrophage population that stains with Annexin V of approximately 16%, a value similar to that of staurosporine, a known apoptosis stimulant (**Fig. 14**). IpgC is unable to cause this phenotype. The population of cells staining with PI is the same percentage as the control with only LDAO (**Fig. 14**).

By using a purified protein model, we were able to assert that IpaD is able to cause cytotoxicity, initiator and effector caspase activation, mitochondrial disruption and Annexin V staining. When all these events are considered in a timeline, we can conclude that the macrophage cell death seen upon exposure to IpaD is occurring through an apoptotic cascade.

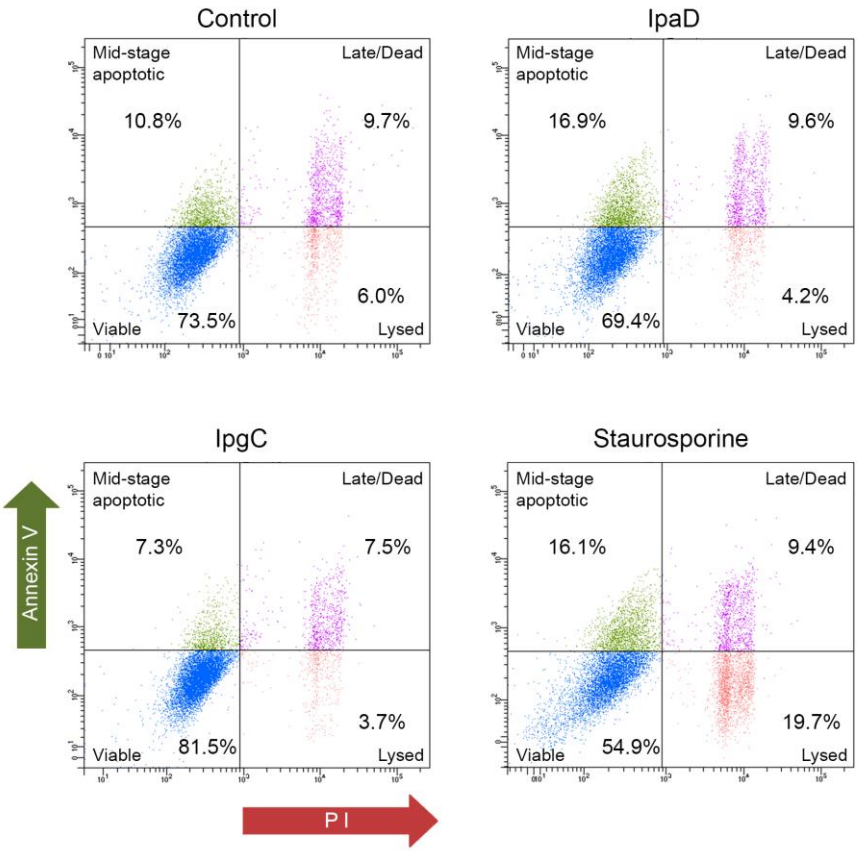

Fig. 14. Apoptosis profiles by exposure to purified proteins. Cells were incubated with LDAO, 2.4 μM IpaD, 2.4 μM IpgC or 1 μM of staurosporine for 1 hour. Annexin V staining indicates cell populations that are in mid-stage apoptosis. Those that have lost their membrane integrity will also exhibit PI staining. Cells that are necrotic only exhibit PI staining.

The role of the mitochondrion in apoptosis is well-documented[101,106,107,107,116,134]. Mitochondrial outer membrane permeabilization is regulated by the Bcl-2 family of proteins, which contains both pro- and anti-apoptotic factors. Disruption of mitochondria results in the detachment and release of Cytochrome C to the cytoplasm, where it is able to activate caspase-9, and it can also activate caspase-2[135,136]. Caspase-2 can also act upstream of cytochrome C and disrupt the mitochondrial membrane directly[137–139]. Loss of mitochondrial membrane potential ($\Delta\Psi m$) can be analyzed with

the fluorescent dye JC-1. This dye is cell-permeable and is able to accumulate both in the cytoplasm, where it exhibits fluorescence at 488 nm (green), and the mitochondria, where it aggregates and fluoresces at 535 nm (red). If the mitochondrion has loss of membrane potential, the red fluorescence will decrease while the cytoplasmic localization remains unchanged. We used JC-1 to investigate if IpaD was able to disrupt the mitochondria. Macrophages incubated with IpaD for 30 minutes, when caspase activation could be initiated according to our previous results show loss of mitochondrial membrane potential (**Fig. 15**). This indicates that IpaD is a factor acting upon the mitochondria resulting in their membrane permeabilization. Furthermore, infection of macrophages with $IpaD^{+}$ for the same amount of time also show loss of mitochondrial membrane potential (approximately 18% of the population) (**Fig. 16**). The $IpaD^{\Delta 41\text{-}80}$ strain shows a reduced ability to disrupt the mitochondria (approximately 9% of the population). Strain $IpaD^{-}$ does not induce any substantial mitochondrial disruption (**Fig. 16**). Thus, the effect of mitochondrial membrane potential loss can be triggered by infection with a strain that shows a complete ability to cause cell death. In turn, a strain mutated in IpaD that is defective in cytotoxicity causes less impact on $\Delta\Psi m$.

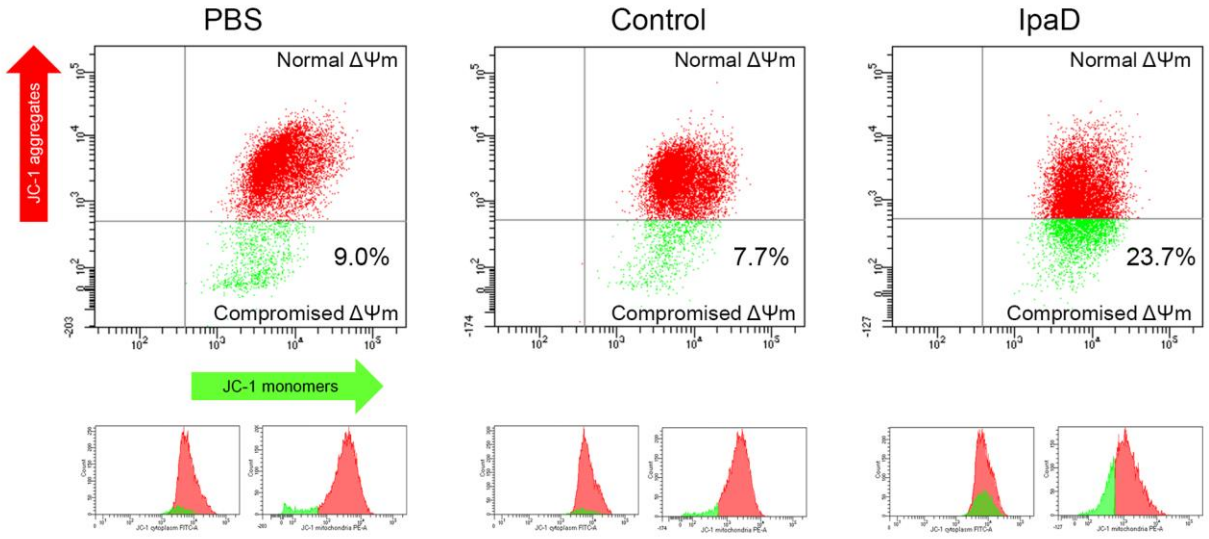

Fig. 15. Mitochondrial damage caused by exposure to IpaD. The labeling of a macrophage population with the dye JC-1 was analyzed by flow cytometry. Red fluorescence indicates JC-1 aggregates that accumulate in the mitochondria. Green fluorescence indicates JC-1 monomers that are found in the cytoplasm. A population losing fluorescence in the red channel is the one losing its mitochondrial membrane potential (ΔΨm). IpaD causes loss of ΔΨm in approximately 24% of the cell population. LDAO (control) has no effect in mitochondria when compared to a PBS control.

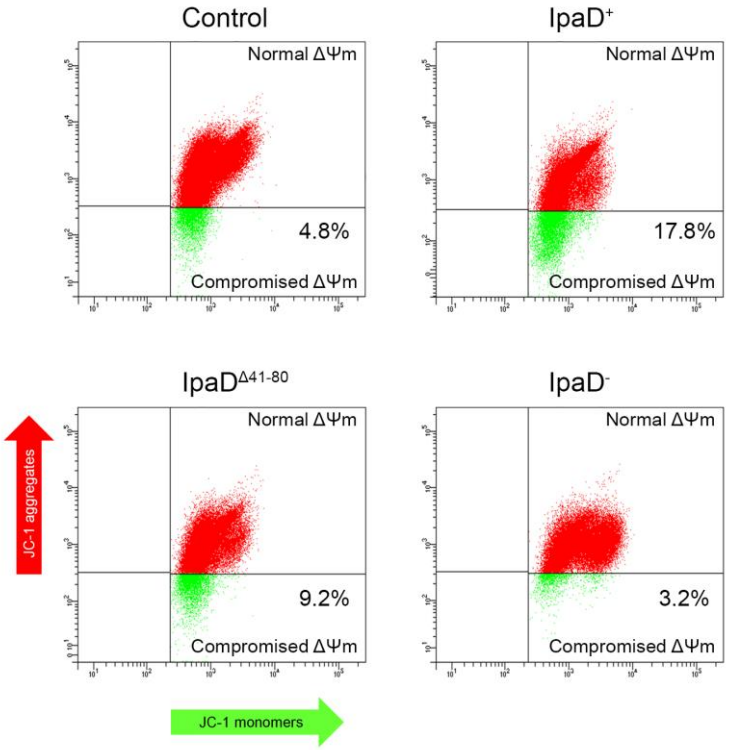

Fig. 16. Mitochondrial damage caused by infection with *S. flexneri* strains. The IpaD$_{+}$ strain causes loss of mitochondrial membrane potential (ΔΨm) in a discrete cell population at 30 minutes post-infection. Cells infected with IpaD$^{\Delta 41\text{-}80}$ show reduced ΔΨm loss. Cells infected with IpaD^{-} do not lose ΔΨm when compared to the control (media only).

Conclusions

Our experiments on *S. flexneri* infection of macrophages demonstrate that caspase-1 activity is not the only trigger of cell death in infected cells and confirm that other caspases are involved. IpaD was identified as a contributing factor to macrophage cell death. We found that IpaD-induced cell death is independent on caspase-1 and -11 and deletion of a region in the N-terminus of IpaD virtually eliminated all cell death not caused by caspase-1 and -11. A point mutant in the same region was also moderately impaired in cytotoxicity. Previous studies have established that IpaD is secreted when the T3SS is induced[89,90]. The effector protein solution released in the *Shigella* culture supernatants stimulated with Congo red indicate that this effect can be seen *in vitro*[79]. Our results seem to indicate that *in vitro*, IpaD is also acting as a molecular signal for macrophage killing.

We performed preliminary *in vitro* studies that show that recombinant IpaD protein is able to elicit apoptosis in macrophages and that this could be used to determine the role of IpaD in the apoptotic death of macrophages, and to infer what could be happening to macrophages infected with *Shigella*. IpaD could be a factor contributing to macrophage cell death upon *Shigella* infection via a caspase-dependent mechanism. During the apoptotic process activated by IpaD, it appears that there is activation of several caspases and a loss of mitochondrial membrane potential ($\Delta\Psi m$). Based on the findings presented here, we propose that IpaD is part of a mitochondrial damage cascade that results in macrophage death, and this event could occur in parallel with pyroptosis.

CHAPTER IV: Analysis of the Effect of IpaD on Cytoskeletal Elements of Epithelial Cells

Introduction

Following invasion of epithelial cells, *Shigella* moves about the cell using actin-based motility with the polarly-located protein IcsA. These bacteria are then able to spread laterally by forming protrusions into adjacent cells and lysing the resulting double membrane vacuoles, an event that is dependent on its T3SS[69]. Indications of a possible effector role for IpaD included the finding that Ipa proteins, including IpaD, are stored in the cytoplasm at levels beyond what is needed for their membrane-bound assemblies and they are released into the medium upon contact with host cells, thereby suggesting they could have effector roles in epithelial cells[86,87,140]. Certain T3SA components are necessary as both effectors and structural components for complete virulence and epithelial cell invasion. The T3SA protein IpaC mediates cytoskeletal rearrangements through an indirect activation of Cdc42/RAC[141,142]. The T3SA protein IpaB in turn acts upon macrophages causing ion channels that trigger death through pyroptosis[64]. IpaB, IpaC and IpaD are needed for intercellular spread of *Shigella*; and a *spa32* null mutant strain was used to show that exposure of IpaB, IpaC and IpaD on the bacterial surface is not enough for an invasive phenotype, rather translocation of these factors is required for pathogenesis[86].

In this project, we were interested in the possible effect of IpaD on elements of the cytoskeleton that promote internalization and intercellular spread of *Shigella*. Since lack of expression of IpaD causes *Shigella* to be avirulent, mutational analyses are challenging and make it difficult for us to study the role of IpaD in invasion and pathogenesis beyond its structural role at the T3SA needle tip. Therefore, we transfected a humanized *ipaD* gene into two different human cell lines and analyzed its expression and effects on these cells through biochemical, microscopic and phenotypic analyses. Ectopically-expressed IpaD appears to co-localize with the cytoskeletal

component F-actin to induce morphological changes. Interaction with vimentin, another cytoskeletal component that functions as an intermediate filament structural protein, was also analyzed. The effect of these observations on phenotypic defects in invasiveness and cell-to-cell spread was also assessed.

Results

An analysis of the expression of IpaD in epithelial cells was performed following transfection with the *ipaD* gene. Transfection of a plasmid harboring the wild-type *ipaD* gene resulted in poor expression of IpaD. In turn, transfection of a humanized *ipaD* (hmn-*ipaD*) gene cloned into a mammalian expression vector allowed us to investigate the preferential localization IpaD could have inside a host epithelial cell. Confocal immunofluorescence of hmn-*ipaD*-transfected HEK-293 cells showed that morphology was altered when compared to mock-transfected cells, starting at 8 hours post-transfection and up to four days later (**Fig. 17**). Changes observed included membrane ruffling and a marked increase in filopodia and lamellipodia. Transfection efficiency was estimated at 40-60%, thus we were able to qualitatively compare cells in the same preparation which were expressing IpaD versus those without apparent expression. Cells expressing IpaD were characteristically more ruffled and their membrane periphery had filamentous extensions of 1-5 µm, whereas cells with no IpaD staining only showed their typical focal adhesions. IpaD appears to be cytosolic as it is found distributed throughout the cell cytoplasm. Additionally, IpaD appears to co-localize with F-actin. The filopodial extensions observed in IpaD-expressing cells are composed of F-actin, as phalloidin stains them across their length. Interestingly, IpaD appears to preferentially localize to the tips of these filaments (**Fig. 17**). In the experiments with cultured macrophages described in Chapter III, Alexa-labeled IpaD was not associated with the cytoskeleton and intracellular localization of the protein affected cell morphology only as a result

of the apoptotic pathway triggered. The contrast between the phenotypes exhibited by epithelial versus macrophage cells could be due to different roles of IpaD in the infective cycle of *Shigella*.

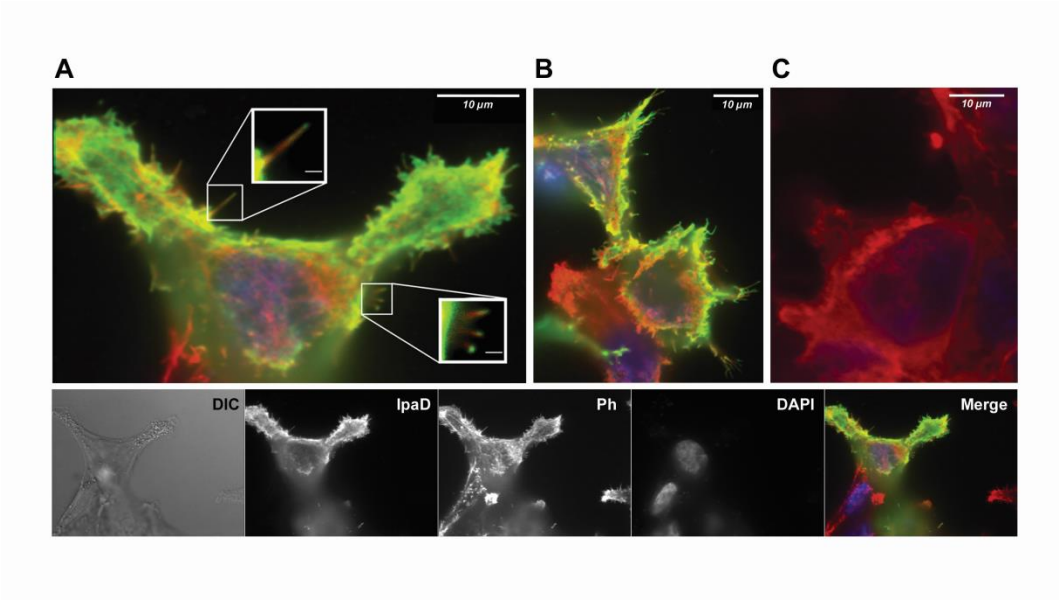

Fig. 17. Immunofluorescence microscopy of hmn-*ipaD*-transfected HEK-293 cells. Morphological changes were observed in cells expressing IpaD vs. mock-transfected cells. Membrane ruffling, increase in filopodial extensions and lamellipodia were seen. In these confocal sections, IpaD (green) displays co-localization with F-actin (red). A and B) Insets show cell projections zoomed in and contrast enhanced to show IpaD and F-actin staining (inset scale bars are 1 µm). IpaD appears to specifically localize to the tips of these filaments. Bottom panels show independent channel signals for A. C) Cells transfected with a mock show no IpaD expression.

We immunoprecipitated IpaD from total protein lysates derived from hmn-*ipaD*-transfected or mock-transfected cells. By performing a cross-linked co-immunoprecipitation, we were able to image the proteins present in the eluates by SDS-PAGE and Oriole staining. Several bands were present in the experimental lysate, along with IpaD whereas no visible bands were found in lanes for immunoprecipitations ran with no antibody, no lysate, control lysate or control lysate spiked with recombinant 6xHis-IpaD (**Fig. 18**). Co-immunoprecipitated proteins were identified by mass spectrometry (LC-MS/MS) for samples equivalent to lanes 1 and 4. Some hits relevant to cytoskeletal rearrangement are presented in **Table 1**.

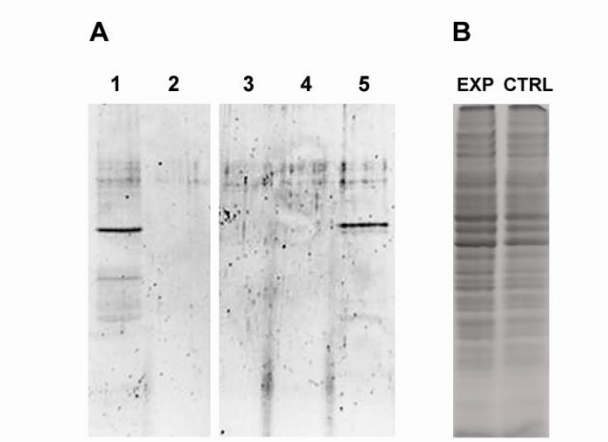

Fig. 18. Co-immunoprecipitation of hmn-ipaD transfected total cell lysates. Co-immunoprecipitation was performed using a purified anti-IpaD polyclonal antibody as bait. A) Lanes 1 through 5 show total protein content eluted from preparations as follows: 1, antibody plus ipaD-transfected cell lysate; 2, no antibody plus ipaD-transfected cell lysate; 3, antibody only; 4, antibody plus mock-transfected cell lysate; 5, antibody plus mock-transfected cell lysate and recombinant 6xHis-IpaD protein. Mass spectrometry by LC-MS/MS was performed on samples corresponding to lanes 1 and 4. B) Total protein lysates. SDS-PAGE of protein lysates prior to use in Co-IP display similar total protein concentration in ipaD-transfected cell lysate (EXP) or mock-transfected cell lysate (CTRL).

Table 1. Hits for cytoskeletal components pulled down with IpaD.

Protein	Function	Fold-increase[1]
IpaD	*S. flexneri* T3SA component	420.5
Vimentin	Structural, intermediate filaments	111.0
Tropomyosin α3	Actin-binding, regulates contraction through myosin binding	34.3
GNB2L1 (Guanine nucleotide-binding protein)	Binds and activates RhoA Binds YopK (*Yersinia* spp.), which inhibits phagocytosis	16.0
Tubulin α	Structural, microtubules	3.0
Actin-2	Structural, microfilaments	2.5
Cofilin-1	Actin-modulating, depolymerizes F-actin, inhibits G-actin polymerization	0.4

[1]Relative abundance of experimental (lysate of *ipaD* transfected cells) vs. control (lysate of mock transfected cells)

To further investigate the morphological changes observed in cells expressing IpaD, we focused on potential interactions of IpaD with components of the cytoskeleton. IpaD co-immunoprecipitated with several cytoskeletal proteins and three major structural components were identified: vimentin, a filamentous protein commonly observed as a tetramer that self-assembles into intermediate filaments; actin-2, an isoform of the core structural element of microfilaments; and tubulin-α, part of the heterodimer that forms microtubules (**Table 1**). Actin-binding proteins were also identified, tropomyosin α3 and cofilin-1. The guanine nucleotide-binding protein GNB2L1 interacts with and activates RhoA, a small GTPase that triggers the formation of actin stress fibers.

Three of the binding partners identified (vimentin, actin and tubulin-α) were confirmed by western-blot analysis of co-immunoprecipitates for IpaD. Furthermore, the specificity of these interactions was tested by performing reverse co-immunoprecipitation, in which the bait was aimed at the binding partner and the presence of IpaD probed. In these, IpaD was found as a strong co-eluate of immunoprecipitation against actin. A discrete portion was a co-eluate in immunoprecipitation against vimentin, but no co-elution was seen in the sample testing against tubulin-α (**Fig. 19**).

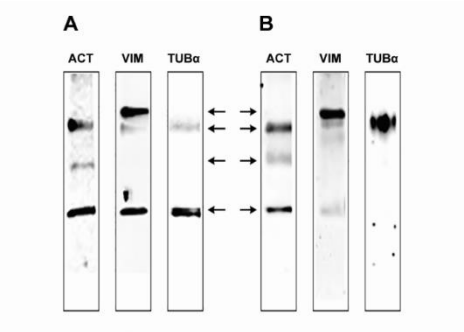

Fig. 19. Co-immunoprecipitation of IpaD-expressing cell total protein lysates. A) Cross-linked co-IP was performed by baiting IpaD and eluates probed by western-blot against potential binding partners. Actin (42 and 53 kDa, second and third arrows), vimentin (57 kDa, first arrow) and tubulin-α (55 kDa, second arrow) were present as co-eluates with IpaD (37 kDa, fourth arrow). B) Reverse co-immunoprecipitation. Cross-linked co-IP was performed by using monoclonal antibodies against the three possible binding partners. IpaD was found in the eluate of co-IPs against actin and vimentin; but not in a co-IP baiting tubulin.

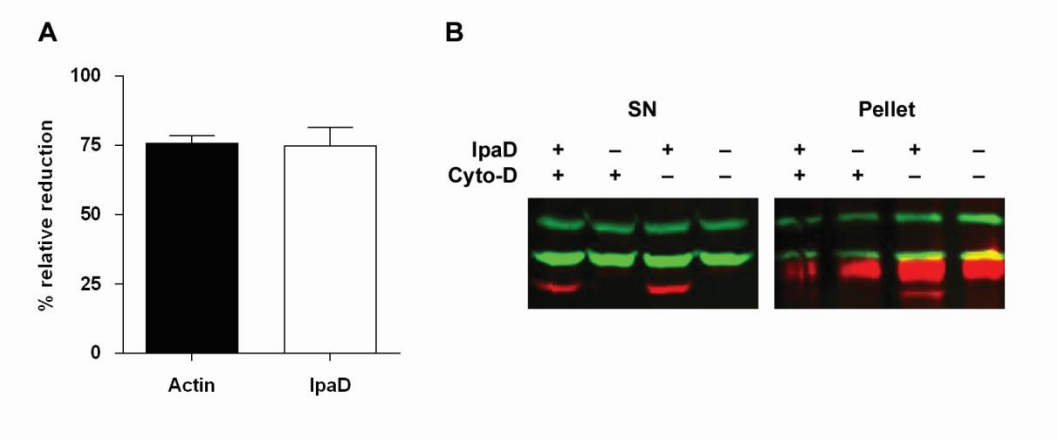

Fig. 20. Actin sedimentation assay. Cell lysates from IpaD-expressing or mock-transfected cells were treated with 10 µM Cytochalasin D (Cyto-D) or left untreated for 1 hour, F-actin and G-actin levels were probed by western-blot. A and B) Densitometric values of the bands corresponding to actin (lower, 42 kDa) and IpaD (37 kDa) were measured for three independent experiments. The band at 40 kDa is non-specific, since it is also present in mock-transfected cells.

In order to further our understanding of the IpaD-actin interaction, we analyzed whether IpaD would preferentially bind globular soluble actin (G-actin) or its filamentous form (F-actin). To achieve this, an actin sedimentation assay was performed, as described previously[143]. A cytoskeleton stabilization buffer and ultracentrifugation are used to isolate the soluble (i.e. cytosolic proteins) or insoluble (F-actin and other cytoskeletal proteins) portions of a cell. In experimental lysates, IpaD was found in both portions, however, treatment with Cytochalasin D (Cyto-D) prior to centrifugation decreases the amount of IpaD in the pellet at the same rate as F-actin perhaps suggesting a preferential association of IpaD to filamentous actin (**Fig. 20**). Treatment with Cyto-D results in a significant difference in the amounts of both proteins, as determined by densitometry (IpaD, p=0.0056; actin, p=0.0010).

Unfortunately, our attempts at establishing a particular phenotype of invasiveness and cell-to-cell spread efficiency of *S. flexneri* in transfected cells were unsuccessful. Furthermore, based on the data obtained thus far, no biologically relevant model could be developed to explain the observations described for this project.

CHAPTER V: Discussion

The purpose of these studies was to expand upon our knowledge of the T3SA protein IpaD, which we found to be secreted following T3SS-induction at levels beyond what would be required for its function only as a needle tip protein. Ménard et al. observed that IpaD was secreted into culture supernatant[87] and later found that this secretion could be activated by proximity to or contact with epithelial cells[144]. Other studies showed similar results with regard to the induced secretion of Ipa proteins, including IpaD[86,145]. Our hypothesis is that the secretion described should correspond with an effector role for IpaD. If secretion of IpaD occurs inside the host cell upon translocon insertion, the bacterium must benefit from injecting this protein in a soluble form into the cytoplasm of the host cell. Translocon partners IpaB and IpaC are also secreted in significant amounts upon T3SS induction (**Fig. 7**) and a distinct effector role has been described for each. IpaB is involved in macrophage death through an inflammatory pathway called pyroptosis, which is initiated by caspase -1[64,111]. IpaC is able to indirectly activate Cdc42/RAC and trigger cytoskeletal rearrangements in epithelial cells[141].

Secretion of IpaD is more efficient when the bacteria are localized at the basolateral surface of polarized Caco-2 cells (an enterocyte cell line), as opposed to their apical side[86]. This observation complements evidence indicating *Shigella* is unable to invade colonic epithelial cells through their apical side[146]. This secretion phenotype would be consistent with the hypothesis that secreted IpaD plays a role in epithelial cell invasion or perhaps the fitness of *Shigella* inside this type of cell. The project described in Chapter IV was based on this hypothesis. The essential role of IpaD in the structure of the T3SA imposes difficulties on the analysis of its role as a secreted effector. Through the use of a transfection system we attempted to identify a role for intracellular IpaD, which would

enable us to study the localization of IpaD inside an epithelial cell and describe possible binding partners.

Although our initial results were suggestive of cytoskeletal rearrangements caused by IpaD (**Fig. 17**, **Fig. 20**), these findings did not correlate to any of the phenotypes assessed. It would be expected that if a particular *Shigella* effector is found in excess in the host cell cytoplasm, this would lead to an effect on bacterial fitness. Given that the changes we were observing with overexpression of IpaD were directed at the cytoskeleton, we hypothesized that these changes would be beneficial to *Shigella* invasiveness or intercellular spread. Unfortunately, assays that looked at invasion and plaque formation in transfected cells showed inconsistent results.

We hypothesize that the high levels of IpaD secreted by *Shigella in vitro* would have to be the result of its active secretion as an effector. Much like IpaB and IpaC, secretion of a protein constitutes energy spent on a benefit to the bacterium. We started our study looking into epithelial cells, proposing that the role of IpaD in the pathogenesis of *Shigella* would be found in their late infective cycle. IpaD has since been shown to induce apoptosis in B lymphocytes, however, we saw no such cell death in cultured epithelial cell lines. The studies looking at secretion of IpaD upon epithelial cell contact did not eliminate the possibility that common components in eukaryotic cells could all trigger the same response, or that many different stimuli could signal the bacterium to unload IpaB, IpaC and IpaD from its cytoplasm. In fact, several types of stimuli have been shown to trigger their secretion, such as serum[144,147], small dye compounds[145], and several components of the extracellular matrix[86]. This opened up the possibility that IpaD might have an effector role in some types of cells, but perhaps not in others.

In the project detailed in Chapter III we utilized murine cells as a model for the study of IpaD secretion in macrophages. Macrophages are cells of the innate immune system that can be found

in the mucosa-associated lymphoid tissue (MALT) of the gastrointestinal tract. It has been observed in both patient biopsies[57] and experimental models[58] that immune cells in the epithelial submucosal region die as a result of infection with *Shigella*. Our first findings showed that this cell death could be due to distinct types of cell death (**Fig. 2**) and that cell death by non-inflammatory caspases could be tied to the functionality of IpaD (**Fig. 3**).

Inflammation is triggered to occur by *Shigella* at the very early stages of infection, when the M cells deliver the bacteria to macrophages in the lamina propria and these are rapidly killed by *Shigella* through pyroptosis. Pyroptosis allows the bacteria to be released onto the basolateral side, where they continue their infective cycle by invading epithelial cells[148], however, ATP release by intestinal epithelial cells leads to further inflammatory signals in the gut. This mechanism is used by the host to expand the localized immune response, including augmented phagocytosis and migration. *S. flexneri* was described to use its effector IpgD to block this inflammatory signal in epithelial cells[149], a sign that *Shigella* modulates the inflammatory processes to its advantage. The interaction between the epithelial layer and the immune cells in the lamina propria of the gut is fundamental to a homeostatic balance that allows this tissue to harbor commensal bacterial flora while defending against pathogenic bacteria[150,151]. One of the mechanisms that ensures proper homeostasis is the ability to balance inflammation[150].

Acute inflammation is necessary for initial *Shigella* dissemination in the colon, as it allows for pathogen escape from macrophages and, ultimately, the destruction of the epithelial barrier promotes bacterial shedding by the host organism[152,153]. This balance between tissue destruction and bacterial advantage was first identified with an *in vitro* system that showed polymorphonuclear leukocytes could migrate towards *S. flexneri*, disrupting a polarized cell monolayer and allowing the bacteria to further infiltrate the submucosa to invade the epithelium[152]. It has since been

described in detail how the symptoms of shigellosis are a result of this inflammatory process[154]. Furthermore, it is thought that *Shigella* is unable to cause an intestinal infection in mice because their acute inflammatory response is different than the human response[155]. Finding that we could uncouple two different types of signals, namely inflammatory and non-inflammatory caspases, prompted us to think that *Shigella* might be able to also modulate the type of cell death that it can cause to host macrophages, and with that, modulate the inflammatory response.

By infecting cultured macrophages, we identified that the cytotoxicity of *Shigella* could be inhibited by small compounds that inhibited caspases, proteases implicated in programmed cell death mechanisms. The inflammatory caspases -1 and -11 had already been studied as components triggered upon *Shigella* infection[65,148] that result in macrophage death by pyroptosis. However, we found that other non-inflammatory caspases could be activated by this infection, opening the possibility that *Shigella* could also kill macrophages through mechanisms yet unidentified. A complemented IpaD^{+} strain was able to activate all caspases, whereas a strain IpaD$^{\Delta 41\text{-}80}$ was only able to activate the inflammatory caspases (**Fig. 3**) and was unable to cause mitochondrial disruption (**Fig. 16**) which is a key element of intrinsic apoptosis. This type of apoptosis occurs by intracellular insults, perhaps like internalized *Shigella* that has escaped from a phagosome. When deletion mutants were used to study the role of IpaD as a regulatory protein in the T3SA, strains with deletions in the N-terminal domain of IpaD had no major impairment in invasiveness or secretion control. Although this same study found that the N-terminal was important for a complete contact hemolysis phenotype, we found that, for IpaD$^{\Delta 41\text{-}80}$ this did not affect its efficiency and survival during macrophage invasion (similar bacterial loads were found in cells infected with IpaD^{+} and IpaD$^{\Delta 41\text{-}80}$, not shown) or phagosomal escape (**Fig. 6**).

An inflammatory type of cell death would be mostly beneficial to the host in promoting pathogen clearance. It might be necessary for *Shigella* to trigger macrophage apoptosis to limit the number of host defensive cells that infiltrate onto the lamina propria. It has been shown that in the inflamed gut, programmed cell death is a way to recover from acute inflammation and return to homeostasis[156]. We believe *Shigella* is controlling the host's apoptosis pathways as a modulatory tactic. If acute inflammation is not resolved, a state of chronic inflammation is reached. Shigellosis can indeed lead to chronic inflammation, as exhibited by the development of Reactive Arthritis (ReA) in certain invididuals. However, this is seen in less than 1% of shigellosis cases, and it has been explained through the observations that those who develop ReA have an HLA-B27 polymorphism[157] and the strains able to cause this autoinflammatory process harbor the plasmid pHS2[158]. Therefore, we do not believe a sustainable state of infection used by *Shigella* is one where inflammation is constant.

The findings described in this dissertation have broader implications for the field of gram-negative bacteria. Exploration of the mechanisms used by *Shigella* to avoid the immune system could potentially lead to new antimicrobials, as targeting conserved virulence targets such as the T3SS components has been proposed before[159,160]. For example, we have shown that IpaD and its structural homologue SipD trigger apoptosis in cultured (and primary, in the case of IpaD) macrophages whereas LcrV does not. These nuances could allow for specificity of the antimicrobials developed. Another avenue of exploration that remains is whether this effect is only seen in enteric pathogens, and the differences perceived depend on the niche to which these proteins have adapted to function in their corresponding bacteria.

Also, further studies are warranted to fully understand the manner in which IpaD starts an apoptotic cascade. With our observations from the project described in Chapter IV, we can conclude that

IpaD does not kill epithelial cells, consistent with the infective cycle of *Shigella* which has been found to utilize mechanisms to actively suppress the death of its epithelial cell host[161]. Our results also indicate that IpaD can only trigger macrophage death when it is localized intracellularly, a factor that acts in this manner would likely trigger intrinsic apoptosis through mitochondrial destabilization. Indeed, our findings include the mitochondrial disruption characteristic of an apoptotic cell with both introduction of purified IpaD and infection with the strain IpaD^{+}. There remains an additional direction to this work, to find if the effect of IpaD is through binding a cytoplasmic partner able to exert changes in the mitochondria such as the pro-apoptotic factors of the Bcl-2 family, or if IpaD itself is able to insert or bind to the mitochondrial membrane. This information would further illustrate for the first time how a T3SS tip protein can interact as an effector within a macrophage cell.

CHAPTER VI: References

1. Centers for Disease Control and Prevention. Global Diarrhea Burden | Global Water, Sanitation and Hygiene | Healthy Water | CDC [Internet]. Available from: http://www.cdc.gov/healthywater/global/diarrhea-burden.html

2. Liu L, Johnson HL, Cousens S, et al. Global, regional, and national causes of child mortality: an updated systematic analysis for 2010 with time trends since 2000. Lancet Lond Engl 2012;379(9832):2151–61.

3. UNICEF, Organización Mundial de la Salud. Diarrhoea: why children are still dying and what can be done. New York: United Nations Children's Fund; 2009.

4. World Health Organization. WHO | Diarrhoeal disease [Internet]. 2013. Available from: http://www.who.int/mediacentre/factsheets/fs330/en/

5. Black RE, Morris SS, Bryce J. Where and why are 10 million children dying every year? Lancet Lond Engl 2003;361(9376):2226–34.

6. Parashar UD, Hummelman EG, Bresee JS, Miller MA, Glass RI. Global illness and deaths caused by rotavirus disease in children. Emerg Infect Dis 2003;9(5):565–72.

7. Gould LH, Walsh KA, Vieira AR, et al. Surveillance for foodborne disease outbreaks - United States, 1998-2008. Morb Mortal Wkly Rep Surveill Summ Wash DC 2002 2013;62(2):1–34.

8. Centers for Disease Control and Prevention. Diagnosis and Management of Foodborne Illnesses --- A Primer for Physicians and Other Health Care Professionals [Internet]. 2004. Available from: http://www.cdc.gov/mmwr/preview/mmwrhtml/rr5304a1.htm

9. Heiman KE, Bowen A. Shigellosis. Cent Dis Control Prev 2014;

10. Bardhan P, Faruque ASG, Naheed A, Sack DA. Decreasing Shigellosis-related Deaths without *Shigella* spp.–specific Interventions, Asia. Emerg Infect Dis 2010;16(11):1718–23.

11. Mazumder RN, Hoque SS, Ashraf H, Kabir I, Wahed MA. Early feeding of an energy dense diet during acute shigellosis enhances growth in malnourished children. J Nutr 1997;127(1):51–4.

12. Keusch GT, Fontaine O, Bhargava A, et al. Diarrheal Diseases [Internet]. In: Jamison DT, Breman JG, Measham AR, et al., editors. Disease Control Priorities in Developing Countries. Washington (DC): World Bank; 2006 [cited 2016 Feb 22]. Available from: http://www.ncbi.nlm.nih.gov/books/NBK11764/

13. Farag TH, Faruque AS, Wu Y, et al. Housefly population density correlates with shigellosis among children in Mirzapur, Bangladesh: a time series analysis. PLoS Negl Trop Dis 2013;7(6):e2280.

14. Khalil K, Lindblom GB, Mazhar K, Kaijser B. Flies and water as reservoirs for bacterial enteropathogens in urban and rural areas in and around Lahore, Pakistan. Epidemiol Infect 1994;113(3):435–44.

15. Huttly SR, Morris SS, Pisani V. Prevention of diarrhoea in young children in developing countries. Bull World Health Organ 1997;75(2):163–74.

16. Martinez-Becerra FJ, Arizmendi O, Greenwood II JC, Picking WL. Development of Subunit Vaccines Against Shigellosis: An Update. In: Molecular Vaccines. New York: Springer; 2013. p. 193–205.

17. Nalini P. NIH-funded researchers begin trial of Shigella vaccine candidates | National Institutes of Health (NIH) [Internet]. [cited 2016 Mar 5];Available from: http://www.nih.gov/news-events/news-releases/nih-funded-researchers-begin-trial-shigella-vaccine-candidates

18. Martinez-Becerra FJ, Chen X, Dickenson NE, et al. Characterization of a Novel Fusion Protein from IpaB and IpaD of Shigella spp. and Its Potential as a Pan-Shigella Vaccine. Infect Immun 2013;81(12):4470–7.

19. ETEC and Shigella vaccine development – Vaccine Development Global Program - PATH [Internet]. [cited 2016 Mar 5];Available from: http://sites.path.org/vaccinedevelopment/diarrhea-rotavirus-shigella-etec/shigella-and-etec-vaccine-development/

20. Kaminski RW, Wu M, Turbyfill KR, et al. Development and Preclinical Evaluation of a Trivalent, Formalin-Inactivated Shigella Whole-Cell Vaccine. Clin Vaccine Immunol 2014;21(3):366–82.

21. Haley CC, Ong KL, Hedberg K, et al. Risk factors for sporadic shigellosis, FoodNet 2005. Foodborne Pathog Dis 2010;7(7):741–7.

22. Arvelo W, Hinkle CJ, Nguyen TA, et al. Transmission risk factors and treatment of pediatric shigellosis during a large daycare center-associated outbreak of multidrug resistant Shigella sonnei: implications for the management of shigellosis outbreaks among children. Pediatr Infect Dis J 2009;28(11):976–80.

23. Garrett V, Bornschlegel K, Lange D, et al. A recurring outbreak of Shigella sonnei among traditionally observant Jewish children in New York City: the risks of daycare and household transmission. Epidemiol Infect 2006;134(6):1231–6.

24. Kapperud G, Rørvik LM, Hasseltvedt V, et al. Outbreak of Shigella sonnei infection traced to imported iceberg lettuce. J Clin Microbiol 1995;33(3):609–14.

25. Thompson CN, Duy PT, Baker S. The Rising Dominance of Shigella sonnei: An Intercontinental Shift in the Etiology of Bacillary Dysentery. PLoS Negl Trop Dis 2015;9(6):e0003708.

26. Fernandez-Prada CM, Venkatesan MM, Franco AA, et al. Molecular epidemiology of Shigella flexneri in a diarrhoea-endemic area of Lima, Peru. Epidemiol Infect 2004;132(2):303–16.

27. Nath R, Saikia L, Choudhury G, Sharma D. Drug resistant Shigella flexneri in & around Dibrugarh, north-east India. Indian J Med Res 2013;137(1):183–6.

28. Casalino M, Nicoletti M, Salvia A, et al. Characterization of endemic Shigella flexneri strains in Somalia: antimicrobial resistance, plasmid profiles, and serotype correlation. J Clin Microbiol 1994;32(5):1179–83.

29. Dutta S, Dutta D, Dutta P, Matsushita S, Bhattacharya SK, Yoshida S. *Shigella dysenteriae* Serotype 1, Kolkata, India. Emerg Infect Dis 2003;9(11):1471–4.

30. Guerin PJ, Brasher C, Baron E, et al. Shigella dysenteriae serotype 1 in west Africa: intervention strategy for an outbreak in Sierra Leone. Lancet Lond Engl 2003;362(9385):705–6.

31. Kernéis S, Guerin PJ, von Seidlein L, Legros D, Grais RF. A Look Back at an Ongoing Problem: Shigella dysenteriae Type 1 Epidemics in Refugee Settings in Central Africa (1993–1995). PLoS ONE 2009;4(2):e4494.

32. Hale TL, Keusch GT. Shigella [Internet]. In: Baron S, editor. Medical Microbiology. Galveston (TX): University of Texas Medical Branch at Galveston; 1996 [cited 2016 Mar 15]. Available from: http://www.ncbi.nlm.nih.gov/books/NBK8038/

33. Fratamico PM, Liu Y, Kathariou S, American Society for Microbiology, editors. Genomes of foodborne and waterborne pathogens. Washington, DC: ASM Press; 2011.

34. Zuo G, Xu Z, Hao B. Shigella Strains Are Not Clones of Escherichia coli but Sister Species in the Genus Escherichia. Genomics Proteomics Bioinformatics 2013;11(1):61–5.

35. Jakhetia R, Verma NK. Identification and Molecular Characterisation of a Novel Mu-Like Bacteriophage, SfMu, of Shigella flexneri. PLOS ONE 2015;10(4):e0124053.

36. Allison GE, Verma NK. Serotype-converting bacteriophages and O-antigen modification in Shigella flexneri. Trends Microbiol 2000;8(1):17–23.

37. DuPont HL, Levine MM, Hornick RB, Formal SB. Inoculum size in shigellosis and implications for expected mode of transmission. J Infect Dis 1989;159(6):1126–8.

38. Furley CW. EAZWV Transmissible Disease Fact Sheet No. 94 SHIGELLOSIS [Internet]. 2002 [cited 2016 Mar 16];Available from: http://www.eazwv.org/sites/default/files/Files/Infectious%20Diseases%20Handbook/Fact%20Sheets/094%20Shigellosis.pdf

39. Jones TC, editor. Nonhuman primates. 2: [...]: with 24 tables. 1. ed. Berlin: Springer; 1993.

40. Murray PR, Baron EJ, editors. Manual of clinical microbiology. 9th ed. Washington, D.C: ASM Press; 2007.

41. Jeong HJ, Jang ES, Han BI, et al. Acanthamoeba: could it be an environmental host of Shigella? Exp Parasitol 2007;115(2):181–6.

42. Saeed A, Abd H, Edvinsson B, Sandström G. Acanthamoeba castellanii an environmental host for Shigella dysenteriae and Shigella sonnei. Arch Microbiol 2009;191(1):83–8.

43. Saeed A, Johansson D, Sandström G, Abd H. Temperature Depended Role of Shigella flexneri Invasion Plasmid on the Interaction with Acanthamoeba castellanii. Int J Microbiol 2012;2012:917031.

44. Bhattacharya D, Bhattacharya H, Thamizhmani R, et al. Shigellosis in Bay of Bengal Islands, India: clinical and seasonal patterns, surveillance of antibiotic susceptibility patterns, and molecular characterization of multidrug-resistant Shigella strains isolated during a 6-year period from 2006 to 2011. Eur J Clin Microbiol Infect Dis 2014;33(2):157–70.

45. Thompson CN, Thieu NTV, Vinh PV, et al. Clinical implications of reduced susceptibility to fluoroquinolones in paediatric Shigella sonnei and Shigella flexneri infections. J Antimicrob Chemother 2016;71(3):807–15.

46. Multidrug-resistant Shigellosis Spreading in the United States | CDC Online Newsroom | CDC [Internet]. [cited 2016 Mar 16];Available from: http://www.cdc.gov/media/releases/2015/p0402-multidrug-resistant-shigellosis.html

47. Bennish ML. Potentially Lethal Complications of Shigellosis. Clin Infect Dis 1991;13(Supplement 4):S319–24.

48. Brodrick R, Sagar J. Toxic megacolon from sexually transmitted Shigella sonnei infection. Int J Colorectal Dis 2012;27(3):415–415.

49. Liu C, Huang Y, Liao C, Chang S, Hsueh P. Rapidly Fatal Bacteremia Caused by *Shigella sonnei* without Preceding Gastrointestinal Symptoms in an Adult Patient with Lung Cancer. Clin Infect Dis 2009;48(11):1635–6.

50. Sharma S, Arora A. Shigella Flexneri bacteremia in adult. J Lab Physicians 2012;4(1):65.

51. Butler T. Haemolytic uraemic syndrome during shigellosis. Trans R Soc Trop Med Hyg 2012;106(7):395–9.

52. Williams KM, Raybourne RB. Demonstration of cross-reactivity between bacterial antigens and class I human leukocyte antigens by using monoclonal antibodies to Shigella flexneri. Infect Immun 1990;58(6):1774–81.

53. Gaston JSH. Shigella induced reactive arthritis. Ann Rheum Dis 2005;64(4):517–8.

54. Ericsson CD, Hatz C, DuPont AW. Postinfectious Irritable Bowel Syndrome. Clin Infect Dis 2008;46(4):594–9.

55. De Hertogh G, Geboes K. Crohn's disease and infections: a complex relationship. MedGenMed Medscape Gen Med 2004;6(3):14.

56. Wassef JS, Keren DF, Mailloux JL. Role of M cells in initial antigen uptake and in ulcer formation in the rabbit intestinal loop model of shigellosis. Infect Immun 1989;57(3):858–63.

57. Islam D, Veress B, Bardhan PK, Lindberg AA, Christensson B. In situ characterization of inflammatory responses in the rectal mucosae of patients with shigellosis. Infect Immun 1997;65(2):739–49.

58. Zychlinsky A, Thirumalai K, Arondel J, Cantey JR, Aliprantis AO, Sansonetti PJ. In vivo apoptosis in Shigella flexneri infections. Infect Immun 1996;64(12):5357–65.

59. Koterski JF, Nahvi M, Venkatesan MM, Haimovich B. Virulent Shigella flexneri causes damage to mitochondria and triggers necrosis in infected human monocyte-derived macrophages. Infect Immun 2005;73(1):504–13.

60. Willingham SB, Bergstralh DT, O'Connor W, et al. Microbial pathogen-induced necrotic cell death mediated by the inflammasome components CIAS1/cryopyrin/NLRP3 and ASC. Cell Host Microbe 2007;2(3):147–59.

61. Suzuki T, Nakanishi K, Tsutsui H, et al. A novel caspase-1/toll-like receptor 4-independent pathway of cell death induced by cytosolic Shigella in infected macrophages. J Biol Chem 2005;280(14):14042–50.

62. Schroeder GN, Jann NJ, Hilbi H. Intracellular type III secretion by cytoplasmic Shigella flexneri promotes caspase-1-dependent macrophage cell death. Microbiology 2007;153(Pt 9):2862–76.

63. Jorgensen I, Miao EA. Pyroptotic cell death defends against intracellular pathogens. Immunol Rev 2015;265(1):130–42.

64. Senerovic L, Tsunoda SP, Goosmann C, et al. Spontaneous formation of IpaB ion channels in host cell membranes reveals how Shigella induces pyroptosis in macrophages. Cell Death Dis 2012;3:e384.

65. Kayagaki N, Stowe IB, Lee BL, et al. Caspase-11 cleaves gasdermin D for non-canonical inflammasome signalling. Nature 2015;526(7575):666–71.

66. Miao EA, Mao DP, Yudkovsky N, et al. Innate immune detection of the type III secretion apparatus through the NLRC4 inflammasome. Proc Natl Acad Sci U A 2010;107(7):3076–80.

67. Jessen DL, Osei-Owusu P, Toosky M, Roughead W, Bradley DS, Nilles ML. Type III secretion needle proteins induce cell signaling and cytokine secretion via Toll-like receptors. Infect Immun 2014;82(6):2300–9.

68. Schroeder GN, Hilbi H. Molecular pathogenesis of Shigella spp.: controlling host cell signaling, invasion, and death by type III secretion. Clin Microbiol Rev 2008;21(1):134–56.

69. Hueck CJ. Type III protein secretion systems in bacterial pathogens of animals and plants. Microbiol Mol Biol Rev MMBR 1998;62(2):379–433.

70. Lan R, Lumb B, Ryan D, Reeves PR. Molecular evolution of large virulence plasmid in Shigella clones and enteroinvasive Escherichia coli. Infect Immun 2001;69(10):6303–9.

71. Schuch R, Maurelli AT. Virulence plasmid instability in Shigella flexneri 2a is induced by virulence gene expression. Infect Immun 1997;65(9):3686–92.

72. Maurelli AT, Baudry B, d'Hauteville H, Hale TL, Sansonetti PJ. Cloning of plasmid DNA sequences involved in invasion of HeLa cells by Shigella flexneri. Infect Immun 1985;49(1):164–71.

73. Prosseda G, Falconi M, Giangrossi M, Gualerzi CO, Micheli G, Colonna B. The virF promoter in Shigella: more than just a curved DNA stretch. Mol Microbiol 2004;51(2):523–37.

74. Kane KA, Dorman CJ. VirB-Mediated Positive Feedback Control of the Virulence Gene Regulatory Cascade of Shigella flexneri. J Bacteriol 2012;194(19):5264–73.

75. Tobe T, Nagai S, Okada N, Adler B, Yoshikawa M, Sasakawa C. Temperature-regulated expression of invasion genes in Shigella flexneri is controlled through the transcriptional activation of the virB gene on the large plasmid. Mol Microbiol 1991;5(4):887–93.

76. Barison N, Lambers J, Hurwitz R, Kolbe M. Interaction of MxiG with the cytosolic complex of the type III secretion system controls Shigella virulence. FASEB J 2012;26(4):1717–26.

77. Martinez-Argudo I, Blocker AJ. The Shigella T3SS needle transmits a signal for MxiC release, which controls secretion of effectors: Regulatory cascade leading to T3SS activation. Mol Microbiol 2010;78(6):1365–78.

78. Morita-Ishihara T, Ogawa M, Sagara H, Yoshida M, Katayama E, Sasakawa C. Shigella Spa33 Is an Essential C-ring Component of Type III Secretion Machinery. J Biol Chem 2006;281(1):599–607.

79. Tamano K, Aizawa S-I, Katayama E, et al. Supramolecular structure of the *Shigella* type III secretion machinery: the needle part is changeable in length and essential for delivery of effectors. EMBO J 2000;19(15):3876–87.

80. Jouihri N, Sory M-P, Page A-L, Gounon P, Parsot C, Allaoui A. MxiK and MxiN interact with the Spa47 ATPase and are required for transit of the needle components MxiH and MxiI, but not of Ipa proteins, through the type III secretion apparatus of Shigella flexneri. Mol Microbiol 2003;49(3):755–67.

81. Epler CR, Dickenson NE, Bullitt E, Picking WL. Ultrastructural analysis of IpaD at the tip of the nascent MxiH type III secretion apparatus of Shigella flexneri. J Mol Biol 2012;420(1-2):29–39.

82. Dickenson NE, Zhang L, Epler CR, Adam PR, Picking WL, Picking WD. Conformational changes in IpaD from Shigella flexneri upon binding bile salts provide insight into the second step of type III secretion. Biochemistry (Mosc) 2011;50(2):172–80.

83. Epler CR, Dickenson NE, Olive AJ, Picking WL, Picking WD. Liposomes Recruit IpaC to the Shigella flexneri Type III Secretion Apparatus Needle as a Final Step in Secretion Induction. Infect Immun 2009;77(7):2754–61.

84. Page AL, Ohayon H, Sansonetti PJ, Parsot C. The secreted IpaB and IpaC invasins and their cytoplasmic chaperone IpgC are required for intercellular dissemination of Shigella flexneri. Cell Microbiol 1999;1(2):183–93.

85. Cherradi Y, Schiavolin L, Moussa S, et al. Interplay between predicted inner-rod and gatekeeper in controlling substrate specificity of the type III secretion system: MxiC-MxiI interaction controls effectors secretion by *Shigella*. Mol Microbiol 2013;87(6):1183–99.

86. Watarai M, Tobe T, Yoshikawa M, Sasakawa C. Contact of Shigella with host cells triggers release of Ipa invasins and is an essential function of invasiveness. EMBO J 1995;14(11):2461–70.

87. Ménard R, Sansonetti PJ, Parsot C. Nonpolar mutagenesis of the ipa genes defines IpaB, IpaC, and IpaD as effectors of Shigella flexneri entry into epithelial cells. J Bacteriol 1993;175(18):5899–906.

88. Picking WL, Nishioka H, Hearn PD, et al. IpaD of Shigella flexneri is independently required for regulation of Ipa protein secretion and efficient insertion of IpaB and IpaC into host membranes. Infect Immun 2005;73(3):1432–40.

89. Espina M, Olive AJ, Kenjale R, et al. IpaD localizes to the tip of the type III secretion system needle of Shigella flexneri. Infect Immun 2006;74(8):4391–400.

90. Schiavolin L, Meghraoui A, Cherradi Y, Biskri L, Botteaux A, Allaoui A. Functional insights into the Shigella type III needle tip IpaD in secretion control and cell contact. Mol Microbiol 2013;88(2):268–82.

91. Turbyfill KR, Mertz JA, Mallett CP, Oaks EV. Identification of epitope and surface-exposed domains of Shigella flexneri invasion plasmid antigen D (IpaD). Infect Immun 1998;66(5):1999–2006.

92. Roehrich AD, Guillossou E, Blocker AJ, Martinez-Argudo I. Shigella IpaD has a dual role: signal transduction from the type III secretion system needle tip and intracellular secretion regulation. Mol Microbiol 2013;87(3):690–706.

93. Zhang L, Wang Y, Olive AJ, et al. Identification of the MxiH needle protein residues responsible for anchoring invasion plasmid antigen D to the type III secretion needle tip. J Biol Chem 2007;282(44):32144–51.

94. Johnson S, Roversi P, Espina M, et al. Self-chaperoning of the type III secretion system needle tip proteins IpaD and BipD. J Biol Chem 2007;282(6):4035–44.

95. Dickenson NE, Arizmendi O, Patil MK, et al. N-terminus of IpaB provides a potential anchor to the Shigella type III secretion system tip complex protein IpaD. Biochemistry (Mosc) 2013;52(49):8790–9.

96. Nothelfer K, Arena ET, Pinaud L, et al. B lymphocytes undergo TLR2-dependent apoptosis upon Shigella infection. J Exp Med 2014;211(6):1215–29.

97. Maurelli AT, Blackmon B, Curtiss R. Loss of pigmentation in Shigella flexneri 2a is correlated with loss of virulence and virulence-associated plasmid. Infect Immun 1984;43(1):397–401.

98. Sasakawa C, Kamata K, Sakai T, Murayama SY, Makino S, Yoshikawa M. Molecular alteration of the 140-megadalton plasmid associated with loss of virulence and Congo red binding activity in Shigella flexneri. Infect Immun 1986;51(2):470–5.

99. Vandenabeele P, Galluzzi L, Vanden Berghe T, Kroemer G. Molecular mechanisms of necroptosis: an ordered cellular explosion. Nat Rev Mol Cell Biol 2010;11(10):700–14.

100. Fuchs Y, Steller H. Live to die another way: modes of programmed cell death and the signals emanating from dying cells. Nat Rev Mol Cell Biol 2015;16(6):329–44.

101. Elmore S. Apoptosis: A Review of Programmed Cell Death. Toxicol Pathol 2007;35(4):495–516.

102. Chipuk JE, Bouchier-Hayes L, Green DR. Mitochondrial outer membrane permeabilization during apoptosis: the innocent bystander scenario. Cell Death Differ 2006;13(8):1396–402.

103. Earnshaw WC, Martins LM, Kaufmann SH. Mammalian caspases: structure, activation, substrates, and functions during apoptosis. Annu Rev Biochem 1999;68:383–424.

104. Hitomi J, Katayama T, Taniguchi M, Honda A, Imaizumi K, Tohyama M. Apoptosis induced by endoplasmic reticulum stress depends on activation of caspase-3 via caspase-12. Neurosci Lett 2004;357(2):127–30.

105. Giorgi C, Bonora M, Missiroli S, et al. Alterations in Mitochondrial and Endoplasmic Reticulum Signaling by p53 Mutants. Front Oncol 2016;6:42.

106. Landes T, Martinou J-C. Mitochondrial outer membrane permeabilization during apoptosis: The role of mitochondrial fission. Biochim Biophys Acta BBA - Mol Cell Res 2011;1813(4):540–5.

107. Brunelle JK, Letai A. Control of mitochondrial apoptosis by the Bcl-2 family. J Cell Sci 2009;122(Pt 4):437–41.

108. Zychlinsky A, Prevost MC, Sansonetti PJ. Shigella flexneri induces apoptosis in infected macrophages. Nature 1992;358(6382):167–9.

109. Fink SL, Cookson BT. Pyroptosis and host cell death responses during Salmonella infection. Cell Microbiol 2007;9(11):2562–70.

110. Hilbi H, Moss JE, Hersh D, et al. Shigella-induced apoptosis is dependent on caspase-1 which binds to IpaB. J Biol Chem 1998;273(49):32895–900.

111. Schroeder GN, Hilbi H. Cholesterol is required to trigger caspase-1 activation and macrophage apoptosis after phagosomal escape of Shigella. Cell Microbiol 2007;9(1):265–78.

112. Broz P, Monack DM. Noncanonical inflammasomes: caspase-11 activation and effector mechanisms. PLoS Pathog 2013;9(2):e1003144.

113. Chanput W, Peters V, Wichers H. THP-1 and U937 Cells [Internet]. In: Verhoeckx K, Cotter P, López-Expósito I, et al., editors. The Impact of Food Bioactives on Health. Cham:

Springer International Publishing; 2015 [cited 2016 Mar 24]. p. 147–59.Available from: http://link.springer.com/10.1007/978-3-319-16104-4_14

114. Nonaka T, Kuwae A, Sasakawa C, Imajoh-Ohmi S. Shigella flexneri YSH6000 induces two types of cell death, apoptosis and oncosis, in the differentiated human monoblastic cell line U937. FEMS Microbiol Lett 1999;174(1):89–95.

115. Majno G, Joris I. Apoptosis, oncosis, and necrosis. An overview of cell death. Am J Pathol 1995;146(1):3–15.

116. Trump BF, Berezesky IK, Chang SH, Phelps PC. The pathways of cell death: oncosis, apoptosis, and necrosis. Toxicol Pathol 1997;25(1):82–8.

117. Clerc PL, Ryter A, Mounier J, Sansonetti PJ. Plasmid-mediated early killing of eucaryotic cells by Shigella flexneri as studied by infection of J774 macrophages. Infect Immun 1987;55(3):521–7.

118. Guichon A, Zychlinsky A. Clinical isolates of Shigella species induce apoptosis in macrophages. J Infect Dis 1997;175(2):470–3.

119. Bando SY, Moreno ACR, Albuquerque JAT, Amhaz JMK, Moreira-Filho CA, Martinez MB. Expression of bacterial virulence factors and cytokines during in vitro macrophage infection by enteroinvasive Escherichia coli and Shigella flexneri: a comparative study. Mem Inst Oswaldo Cruz 2010;105(6):786–91.

120. Yu J, Oragui EE, Stephens A, Kroll JS, Venkatesan MM. Inactivation of DsbA alters the behaviour of Shigella flexneri towards murine and human-derived macrophage-like cells. FEMS Microbiol Lett 2001;204(1):81–8.

121. Nonaka T, Kuwabara T, Mimuro H, Kuwae A, Imajoh-Ohmi S. Shigella-induced necrosis and apoptosis of U937 cells and J774 macrophages. Microbiology 2003;149(Pt 9):2513–27.

122. Hilbi H, Puro RJ, Zychlinsky A. Tripeptidyl Peptidase II Promotes Maturation of Caspase-1 in Shigella flexneri-Induced Macrophage Apoptosis. Infect Immun 2000;68(10):5502–8.

123. Kuwae A. Shigella Invasion of Macrophage Requires the Insertion of IpaC into the Host Plasma Membrane. FUNCTIONAL ANALYSIS OF IpaC. J Biol Chem 2001;276(34):32230–9.

124. Stevens MP, Wood MW, Taylor LA, et al. An Inv/Mxi-Spa-like type III protein secretion system in Burkholderia pseudomallei modulates intracellular behaviour of the pathogen. Mol Microbiol 2002;46(3):649–59.

125. Zhang J, Jiang R, Wang W, Takayama H, Tanaka Y. Apoptosis are induced in J774 macrophages upon phagocytosis and killing of Pseudomonas aeruginosa. Cell Immunol 2013;286(1-2):11–5.

126. Habyarimana F, Swearingen MC, Young GM, Seveau S, Ahmer BMM. Yersinia enterocolitica inhibits Salmonella enterica serovar Typhimurium and Listeria monocytogenes cellular uptake. Infect Immun 2014;82(1):174–83.

127. Hulme SD, Barrow PA, Foster N. Inhibited Production of iNOS by Murine J774 Macrophages Occurs via a phoP-Regulated Differential Expression of NFκB and AP-1. Interdiscip Perspect Infect Dis 2012;2012:483170.

128. Ekert PG, Silke J, Vaux DL. Caspase inhibitors. Cell Death Differ 1999;6(11):1081–6.

129. Sansonetti PJ, Phalipon A, Arondel J, et al. Caspase-1 activation of IL-1beta and IL-18 are essential for Shigella flexneri-induced inflammation. Immunity 2000;12(5):581–90.

130. Taylor JE, Fernandez-Patron C. Delivery of bioactive, gel-isolated proteins into live cells. Electrophoresis 2003;24(9):1331–7.

131. Espina M, Ausar SF, Middaugh CR, Picking WD, Picking WL. Spectroscopic and calorimetric analyses of invasion plasmid antigen D (IpaD) from Shigella flexneri reveal the presence of two structural domains. Biochemistry (Mosc) 2006;45(30):9219–27.

132. Chatterjee S, Zhong D, Nordhues BA, Battaile KP, Lovell S, De Guzman RN. The crystal structures of the Salmonella type III secretion system tip protein SipD in complex with deoxycholate and chenodeoxycholate. Protein Sci 2011;20(1):75–86.

133. Boatright KM, Salvesen GS. Mechanisms of caspase activation. Curr Opin Cell Biol 2003;15(6):725–31.

134. Costantini P, Bruey JM, Castedo M, et al. Pre-processed caspase-9 contained in mitochondria participates in apoptosis. Cell Death Differ 2002;9(1):82–8.

135. Slee EA, Harte MT, Kluck RM, et al. Ordering the cytochrome c-initiated caspase cascade: hierarchical activation of caspases-2, -3, -6, -7, -8, and -10 in a caspase-9-dependent manner. J Cell Biol 1999;144(2):281–92.

136. Samraj AK, Sohn D, Schulze-Osthoff K, Schmitz I. Loss of caspase-9 reveals its essential role for caspase-2 activation and mitochondrial membrane depolarization. Mol Biol Cell 2007;18(1):84–93.

137. Paroni G, Henderson C, Schneider C, Brancolini C. Caspase-2 can trigger cytochrome C release and apoptosis from the nucleus. J Biol Chem 2002;277(17):15147–61.

138. Robertson JD, Enoksson M, Suomela M, Zhivotovsky B, Orrenius S. Caspase-2 acts upstream of mitochondria to promote cytochrome c release during etoposide-induced apoptosis. J Biol Chem 2002;277(33):29803–9.

139. Enoksson M, Robertson JD, Gogvadze V, et al. Caspase-2 Permeabilizes the Outer Mitochondrial Membrane and Disrupts the Binding of Cytochrome *c* to Anionic Phospholipids. J Biol Chem 2004;279(48):49575–8.

140. Watarai M, Tobe T, Yoshikawa M, Sasakawa C. Disulfide oxidoreductase activity of Shigella flexneri is required for release of Ipa proteins and invasion of epithelial cells. Proc Natl Acad Sci U S A 1995;92(11):4927–31.

141. Tran Van Nhieu G, Caron E, Hall A, Sansonetti PJ. IpaC induces actin polymerization and filopodia formation during Shigella entry into epithelial cells. EMBO J 1999;18(12):3249–62.

142. Terry CM, Picking WL, Birket SE, et al. The C-terminus of IpaC is required for effector activities related to Shigella invasion of host cells. Microb Pathog 2008;45(4):282–9.

143. Kim J, Swee M, Parks WC. Cytosolic SYT/SS18 Isoforms Are Actin-Associated Proteins that Function in Matrix-Specific Adhesion. PLoS ONE 2009;4(7):e6455.

144. Ménard R, Sansonetti P, Parsot C. The secretion of the Shigella flexneri Ipa invasins is activated by epithelial cells and controlled by IpaB and IpaD. EMBO J 1994;13(22):5293–302.

145. Bahrani FK, Sansonetti PJ, Parsot C. Secretion of Ipa proteins by Shigella flexneri: inducer molecules and kinetics of activation. Infect Immun 1997;65(10):4005–10.

146. Mounier J, Vasselon T, Hellio R, Lesourd M, Sansonetti PJ. Shigella flexneri enters human colonic Caco-2 epithelial cells through the basolateral pole. Infect Immun 1992;60(1):237–48.

147. Mounier J, Bahrani FK, Sansonetti PJ. Secretion of Shigella flexneri Ipa invasins on contact with epithelial cells and subsequent entry of the bacterium into cells are growth stage dependent. Infect Immun 1997;65(2):774–82.

148. Suzuki T, Franchi L, Toma C, et al. Differential regulation of caspase-1 activation, pyroptosis, and autophagy via Ipaf and ASC in Shigella-infected macrophages. PLoS Pathog 2007;3(8):e111.

149. Puhar A, Tronchère H, Payrastre B, Tran Van Nhieu G, Sansonetti PJ. A Shigella Effector Dampens Inflammation by Regulating Epithelial Release of Danger Signal ATP through Production of the Lipid Mediator PtdIns5P. Immunity 2013;39(6):1121–31.

150. Ashida H, Ogawa M, Kim M, Mimuro H, Sasakawa C. Bacteria and host interactions in the gut epithelial barrier. Nat Chem Biol 2011;8(1):36–45.

151. Peterson LW, Artis D. Intestinal epithelial cells: regulators of barrier function and immune homeostasis. Nat Rev Immunol 2014;14(3):141–53.

152. Perdomo JJ, Gounon P, Sansonetti PJ. Polymorphonuclear leukocyte transmigration promotes invasion of colonic epithelial monolayer by Shigella flexneri. J Clin Invest 1994;93(2):633–43.

153. Perdomo OJ, Cavaillon JM, Huerre M, Ohayon H, Gounon P, Sansonetti PJ. Acute inflammation causes epithelial invasion and mucosal destruction in experimental shigellosis. J Exp Med 1994;180(4):1307–19.

154. Sansonetti PJ. Rupture, invasion and inflammatory destruction of the intestinal barrier by Shigella: the yin and yang of innate immunity. Can J Infect Dis Med Microbiol J Can Mal Infect Microbiol Médicale AMMI Can 2006;17(2):117–9.

155. Phalipon A, Sansonetti PJ. Shigella's ways of manipulating the host intestinal innate and adaptive immune system: a tool box for survival? Immunol Cell Biol 2007;85(2):119–29.

156. Nunes T, Bernardazzi C, de Souza HS. Cell Death and Inflammatory Bowel Diseases: Apoptosis, Necrosis, and Autophagy in the Intestinal Epithelium. BioMed Res Int 2014;2014:1–12.

157. Colmegna I, Cuchacovich R, Espinoza LR. HLA-B27-associated reactive arthritis: pathogenetic and clinical considerations. Clin Microbiol Rev 2004;17(2):348–69.

158. Adam T, Siewerdt R, Offermann I, et al. Prevalence and molecular diversity of pHS-2 plasmids, marker for arthritogenicity, among clinical Escherichia coli Shigella isolates. Microbes Infect 2003;5(7):579–92.

159. Duncan MC, Linington RG, Auerbuch V. Chemical Inhibitors of the Type Three Secretion System: Disarming Bacterial Pathogens. Antimicrob Agents Chemother 2012;56(11):5433–41.

160. Clatworthy AE, Pierson E, Hung DT. Targeting virulence: a new paradigm for antimicrobial therapy. Nat Chem Biol 2007;3(9):541–8.

161. Kobayashi T, Ogawa M, Sanada T, et al. The Shigella OspC3 Effector Inhibits Caspase-4, Antagonizes Inflammatory Cell Death, and Promotes Epithelial Infection. Cell Host Microbe 2013;13(5):570–83.

CHAPTER VII: Appendices

Appendix A: Solutions

Agarose gel for DNA electrophoresis

25 ml 1X TAE

15 µl 6 mM Ethidium bromide

0.3 g agarose (electrophoresis grade)

1X TAE (running buffer for agarose gel electrophoresis)

4.84g Tris

1.142ml Glacial acetic acid

2ml 0.5 M EDTA

Q.S. to 1 L

Phosphate-Buffered Saline (PBS)

130 mM NaCl

10 mM Na_2HPO_4

1.5 mM K_2HPO_4

3 mM KCl

Q binding buffer

10 mM NaCl

10 mM Na_2HPO_4

Q elution buffer

1 M NaCl

10 mM Na_2HPO_4

12% SDS-PAGE Separating Gel (Sufficient for two gels)

3.00 ml diH20

2.50 ml 1.5 M Tris-HCl, pH 8.8

100 µl 10% (w/v) SDS

4.00 ml 29:1% (w/v) acrylamide:bisacrylamide

0.15 ml 10% (w/v) ammonium persulfate (APS)

10 µl N,N,N′,N′-Tetramethylethylenediamine (TEMED)

15% SDS-PAGE Separating Gel (Sufficient for two gels)

2.50 ml diH20

2.50 ml 1.5 M Tris-HCl, pH 8.8

100 µl 10% (w/v) SDS

5.00 ml 29:1% (w/v) acrylamide:bisacrylamide

0.15 ml 10% (w/v) APS

10 µl TEMED

5% SDS-PAGE Stacking Gel (Sufficient for two gels)

2.85 ml diH2O

1.25 ml 0.5 M Tris-HCl, pH 6.8

50.0 µl 10% (w/v) SDS

1.00 ml 29:1% (w/v) acrylamide:bisacrylamide

0.2ml 10% (w/v) APS

15µl TEMED

SDS-PAGE destain

5% (v/v) methanol

7.5% (v/v) glacial acetic acid

SDS-PAGE running buffer

2.42g Tris

14.41g glycine

1.0g SDS

Q.S. to 1 L

SDS-PAGE stain

0.1% (w/v) Coomassie Brilliant Blue R-250

5% (v/v) methanol

7.5% (v/v) glacial acetic acid

Media:

AI media

1 L of ZY media (10 g tryptone, 5 g yeast extract)

2 ml of 1 M $MgSO_4$

20 ml of 50X 5052

50 ml of 20X NPS

1 M $MgSO_4$

24.65 g MgSO4-7H2O

87 ml H_2O

50X 5052 (100 ml)

25 g glycerol (weigh in beaker)

73 ml H_2O

2.5 g glucose

10 g α-lactose monohydrate

20X NPS (1L):

(NPS = 100 mM PO_4, 25 mM SO_4, 50 mM NH_4, 100 mM Na, 50 mM K)

In a graduated cylinder, combine (in the below sequence) and stir until dissolved:

800 ml nanopure H_2O

66 g $(NH_4)_2SO_4$

136 g KH_2PO_4

142 g Na_2HPO_4

Q.S. to 1 L

Congo Red agar

37g Tryptic soy agar

0.03% Congo Red

Q.S. to 1 L

Luria-Bertani (LB) Broth

25.0 g LB broth (ready-made mix)

Q.S. to 1 L

LB Agar

37.0 g LB agar (ready-made mix)

Q.S. to 1 L

Dulbecco's Modified Eagle Medium (DMEM)

9.53g DMEM

2.2g $NaHCO_3$

Q.S. to 1 L and filter sterilize

Minimal Medium:

This bacterial growth medium provides a non-inducing, lactose-free environment and is excellent for starter (10 ml) cultures for protein expression.

9.25 ml sterile H_2O

20 µl 1 M $MgSO_4$

125 µl 40% glucose

100 µl 25% aspartate

500 µl 20x NPS

Tryptic Soy Agar (TSA)

37g TSA (ready-made mix)

Q.S. to 1 L

Tryptic Soy Broth (TSB)

25g TSB (ready-made mix)

Q.S. to 1 L

Appendix B: Abbreviations

A, Abs	Absorbance
BCA	Bicinchoninic Acid
MOI	Multiplicity of Infection
CFU	Colony-Forming Units
LDH	Lactate Dehydrogenase
BCA	Bicinchoninic Acid
BSA	Bovine Serum Albumin
CD	Circular Dichroism
CFU	Colony-Forming Units
CR	Congo red
Cyto-D	Cytochalasin D
DAPI	4',6-diamidino-2-phenylindole
DMEM	Dulbecco's Modified Eagle Medium
DMF	Dimethylformamide
DMSO	Dimethyl sulfoxide
DTT	Dithiothreitol
E. coli	*Escherichia coli*

EDTA	Disodium ethylenediamine tetraacetate
FITC	Fluorescein-5-isothiocyanate
IgG	Immunoglobulin G
IL	Interleukin
Ipa	Invasion plasmid antigen
kb	Kilobase
kDa	KiloDaltons
LB	Luria-Bertani Broth
LDAO	N,N-Dimethyldodecylamine N-oxide
LDH	Lactate DeHydrogenase
LPS	Lipopolysaccharide
M	Molar
min.	Minute
MOI	Multiplicity of Infection
MW	Molecular weight
PBS	Phosphate-Buffered Saline
PS	Phosphatidylserine
PVDF	Polyvinylidene difluoride

RBC	Red blood cell
RIPA	Radioimmunoprecipitation Assay Buffer
RPMI	Roswell Park Memorial Institute media - 1640
S. flexneri	*Shigella flexneri*
SDS-PAGE	Sodium dodecyl sulfate-polyacrylamide gel electrophoresis
spp.	Species
T3SS	Type III Secretion System
TAE	Tris Acetate EDTA buffer
TBS	Tris-buffered saline
TEMED	N,N,N,N,-tetra-methylethylenediamine
TSA	Trypticase Soy Agar
TSA-CR	Trypticase Soy Agar with 0.025% Congo red
TSB	Trypticase Soy Broth

Appendix C: Purification method for IpaD without any tag

Frozen stock

IpaD no tag / pET9a	Stock #32D6

Culture growth

In 1L AI media

Add 2 ml 1M $MgSO_4$, 50 ml 20X NPS and 20 ml 50X 5052, 1 ml Kanamycin 50 mg/ml

ÄKTA method

Column	Hi-Trap Q FF 5 ml
Buffer A	10mM Tris 10mM NaCl pH 7.5
Buffer B (elution)	10mM Tris 1M NaCl pH 7.5

Steps

Equilibrate column with 5 CV

Injection of SN is with sample pump

Wash with 10 CV

Linear gradient for elution 28% in 21 CV

Elute in 5 ml fractions

Clean w 5 CV B

Reequilibrate with 5 CV A

Repeat steps, loading FT over column until fractions are clean (5th run onwards)

Faster cleanup if half of the culture SN loaded onto column

Approximate yield 20-50 mg/L

Calculate protein concentration

MW = 36690 Da ε = 36900